Joint Wireless Transfer of Information and Energy in Cooperative Relay Networks

Thesis submitted in partial fulfillment
of the requirements for the degree of

Masters of Science
in
Electronics and Communications Engineering
By Research

M. PRUDHVI DEEP
201331045
mutyala.prudhvideep@research.iiit.ac.in

International Institute of Information Technology
Hyderabad - 500 032, INDIA
December 2018

International Institute of Information Technology
Hyderabad, India

CERTIFICATE

It is certified that the work contained in this thesis, titled " Joint Wireless Transfer of Information and Energy in Cooperative Relay Networks " by M. Prudhvi Deep, has been carried out under my supervision and is not submitted elsewhere for a degree.

_____ _____

Date Adviser: Dr. P. Ubaidulla

To

JOE STRUMMER

Acknowledgments

I would like to extend my gratitude to all the people who helped me in completing this work, especially to Apuroop, Vishnu, Abhilash, and Shubham for their counsel.

Abstract

Wireless devices are typically powered by batteries to ensure their portability. The finite energy storage capacity of the batteries limits operational period of the network. Recharging and replacing batteries of devices is time consuming or expensive, particularly when the sensors are deployed in hostile or hard-to-access environments. Energy harvesting (EH), a technique to collect energy from the ambient energy sources including radio frequency (RF) signals, has received considerable attention as a viable solution to this problem. Simultaneous wireless information and energy transfer (SWIET) explores a dual use of RF signals to transfer information jointly with energy using the same waveform. This can guarantee a reliable supply of energy unlike the case of other ambient energy sources.

In this work, we consider SWIET in a cooperative wireless network involving two transceiver nodes whose communication is assisted by energy-constrained two-way amplify-and-forward (AF) relay nodes. The transceiver nodes can simultaneously transmit information and energy, and the relay nodes harvest the energy from the received signal and use the harvested energy to amplify and retransmit the received signal to the transceiver nodes. We consider two practical receiver architectures, namely, time switching (TS) and power splitting (PS). In TS, the receiver harvests energy for a fraction of transmission block and then decodes information for the remaining fraction. In PS, a fraction of the received signal is used for energy harvesting and the rest for information decoding. Based on the TS and PS receiver architectures, we propose the TSR and PSR protocols to facilitate simultaneous energy harvesting and information processing at the relay. For both protocols, we address the problem of resource allocation along with energy harvesting and optimal relay selection. The performance of the proposed PSR and TSR protocols for different parameters is illustrated by numerical simulations.

We extend the relaying protocols discussed above to a cognitive radio (CR) scenario. Cognitive radio networks (CRNs) achieve better spectral efficiency by allowing the licensed users to share their spectrum with unlicensed users. The interference produced by the unlicensed users is kept below an accepted threshold. We consider a CRN with a licensed primary user (PU), two secondary transceivers, and a set of secondary two-way amplify and forward (AF) relays. The secondary user (SU) nodes share the spectrum with the PU node, and each node is assumed to be equipped with a single antenna. SU transceivers communicate with each other only via the relay optimally selected from the set of available relays. The transmit signals from the SU transceivers are designed so as to carry both information and energy. The relay harvests energy from these signals and uses this energy to process the received signals for further transmission.

Contents

List of Figures

List of symbols

α	Time Switching Ratio
ρ	Power Splitting Ratio
η	Energy Harvesting Efficiency
$\mathbb{E}\{\cdot\}$	Expectation Operator
L	Number of relays
T_k	Transceiver k, Here k = 1,2
δ_i	AWGN noise at the ith relay
h_i	Channel gain from T_1 to the ith relay
g_i	Channel gain from T_2 to the ith relay
w_i	Amplification factor or weight coefficient of the ith relay
ϕ_k	AWGN noise at transceiver k
P_{R_i}	Transmit power of the ith relay
R_i	Instantaneous achievable rate of the network
P_T	Total transmit power of the two transceiver nodes T_1 and T_2
θ	Minimum amount of the energy harvested at the relay
γ_i	Interference resulting from the PU transmission at the ith relay
ϵ	Maximum interference produced due to SU transmission that PU can tolerate

ll

List of Acronyms

EH	Energy Harvesting
RF	Radio Frequency
SWIET	Simultaneous wireless information and energy transfer
AF	Amplify and Forward
TS	Time Switching
PS	Power Splitting
TSR	Time Switching based Relaying
PSR	Power Splitting based Relying
CRN	Cognitive Radio Network
PU	Primary User
SU	Secondary User
WCRN	Wireless Cooperative Relaying Network
WSN	Wireless Sensor Network
WET	Wireless Energy Transfer
DC	Direct Current
AC	Alternating Current
EM	Electro Magnetic
EMF	Electromotive force
RIC	Resonant Inductive Coupling
SISO	Single Input Single Output
MIMO	Multiple Input Multiple Output
ID	Information Decoding
CSI	Channel State Information
SINR	Signal to Noise Interference Ratio
AWGN	Additive White Gaussian Noise
DF	Decode and Forward
KKT	Karush–Kuhn–Tucker conditions
WPT	Wireless Power Transfer

ll

Chapter *1*

Introduction

To prolong the lifespan of the energy-constrained nodes, one solution is to harvest ambient energy such as solar, wind, vibrations, etc. However, such sources may not be continuously available and often suffer from low reliability. A more controlled and reliable energy transfer and harvesting can be effected by the electromagnetic field variations induced by nodes having access to a continuous energy supply; this is known as wireless energy transfer (WET). WET techniques can be classified into two categories, namely, non-radiative and radiative. Non-radiative WET utilizes the principle of magnetic induction to transfer energy. This requires proper alignment of coils at the transmitters and receivers. It is not possible to achieve this alignment if the devices in a network are located in remote areas. Therefore, it is often employed for short range WET. In radiative WET, we use electromagnetic (EM) radiation to transfer energy from source to destination. WET using Radio-frequency (RF) signals is a far field energy transfer technique and it is ideally suited to supply energy to a network with a large number of nodes spread over a wide area. However, the transmitted signals should be beamformed in order to achieve better efficiency.

RF waves can be used to transmit energy and information simultaneously. This process of merging WET with information transfer is known as simultaneous wireless information and energy transfer (SWIET). Compared to conventional EH methods, SWIET is less dependent on the surrounding environment. Therefore, SWIET has been proposed as a promising solution to prolong the lifetime of energy constrained nodes. In the earlier studies an ideal SWIET receiver was assumed to process the information and extract energy from the received signal [1, 2]. This assumption may not hold in practice [3], as circuits used for harvesting energy from RF signals are not yet able to decode the carried information directly. Therefore, two practical receiver architectures, namely, time switching (TS) and power splitting (PS) were proposed in [4, 5]. In TS, the receiver harvests energy from the received signal for a fraction of time period and then decodes information for the remaining fraction. In PS, the total power of the signal is split into two parts such that one part is used for energy harvesting and the other for information decoding.

With WET/SWIET, we find an attractive approach to increase the lifespan of the nodes in a network. However, this is not sufficient; the current standards of wireless communication also address the issue of

network coverage and reliability by cooperate relaying. Relays are the intermediate devices introduced in a network to help realize the communication between nodes that are separated by a distance that would make the direct communication impossible. The relays receive the transmission from the source node and retransmit the modified version to the destination. In doing so, they enhance communication range and diversity. Depending on the ability of the relay to regenerate or decode the signals from the terminals, several transmission protocols have been studied. The regenerative relay adopts the decode-and-forward (DF) protocol and performs the decoding process at the relay [6]. The non-regenerative relay typically adopts a form of amplify-and-forward (AF) protocol and does not perform decoding at the relay, but amplifies the signals to retransmit them back to the terminals [7, 8]. Owing to its increased spectral efficiency, two-way relaying scheme turns out to be a better option compared to its one-way counterpart in spectrally-constrained networks [9]. Recently, TS-based relaying (TSR) and PS-based relaying (PSR) have been proposed to utilize the SWIET technique in cooperative relaying networks [10], [11, 12, 13].

To meet the demand for high data rates and to support a large number of users, effective use of spectrum and energy resources is recommended. Cooperative cognitive networks boost the spectrum utilization by allowing the licensed users to share their spectrum with unlicensed users in overlay, underlay, or interweave cognitive radio scenarios. In cognitive radio networks (CRN), there are two types of users, namely the primary user (PU) who has access to the licensed spectrum, and the secondary user (SU) who is allowed to access the licensed spectrum, provided the interference produced at the PU is kept below a threshold. For the interweave mode, SU is allowed to access the licensed spectrum only when the PU is idle. For the underlay mode, the SU can transmit simultaneously with PU, provided the interference at the primary receiver is kept below a threshold. For the overlay mode, PUs and SUs are allowed to transmit simultaneously, provided the SUs assist the PUs transmission. SWIET enabled cooperative cognitive radio networks can guarantee a better utilization of spectrum and energy resources allocated to the network. In Chapter 4, we consider a SWIET enabled underlay CRN, and address the problem of resource allocation and relay selection in the context of rate maximization.

In this thesis, we integrate SWIET into the framework of modern wireless communication networks. First, we consider a wireless cooperative relaying network. We consider practical receiver architectures to support SWIET at the relays. For this network, we address the problem of optimal resource allocation and relay selection. Next, we consider SWIET in a cooperative CRN, operating in underlay mode. Here, the resource allocation and relay selection problem has to be addressed with an additional constraint on PU interference.

1.1 Problem Overview

In this work, we study the performance of a wireless cooperative relaying network (WCRN) and a cognitive radio network (CRN) with added SWIET functionality. The total rate of a network is a quantifiable parameter, and it is used in this work to compare the performance of the networks. The rate

maximization problem in a WCRN turns out to be mixed integer optimization problem which is hard to solve as it is. Instead of tackling this problem head-on, we resolve this problem into two parts. The first part addresses the resource allocation problem and the next one address the relay selection in the network. The same rate maximization problem in a cooperative CRN has an additional constraint on PU interference, and this gives rise to new challenges when compared to the rate maximization problem in the relaying network. The focus of this work rests around providing suitable solutions to the rate maximization problem, for the networks mentioned above, and comparing the rates achieved by these networks for different relaying protocols.

1.2 Contribution

In this thesis, we focus our attention on SWIET enabled wireless networks. First, we consider a wireless cooperative relaying network. The relay employs AF scheme to amplify and transmit the signals to their respective destination. We propose two relaying protocols, namely, TSR and PSR to support energy harvesting and information processing at the relays. We propose an optimization problem to maximize the sum-rate of this network subject to energy harvesting and transmit power constraints for both the protocols. This compound problem is split into two parts, viz, resource allocation and relay selection. For PSR protocol, we make an approximation on the objective of the resource allocation problem, to convert it to a convex optimization problem. We solve the Lagrangian associated with this problem to obtain the closed form solutions. For TSR protocol, we propose an iterative solution to solve the resource allocation problem. The relay selection problem simply boils down to selecting the relay that gives the maximum rate while operating with the transmit powers obtained by solving the resource allocation problem.

Next, we consider SWIET in a cooperative CRN operating in underlay mode. The communication of SUs is aided by a set of AF two-way relays. For PSR and TSR protocols, we formulate an optimization problem to maximize the sum-rate of the network. We address this optimization problem with respect to energy harvesting, transmit power, and PU interference constraints. We solve the resource allocation problem first and then address the relay selection problem. To solve the resource allocation problem for PSR protocol, we relax the constraints on transmit power and solve the resulting sub-problem with energy harvesting and interference constraints. The final solution can be obtained by imposing the transmit power limits on the results of the sub-problem. For TSR protocol, the solution for resource allocation is not direct. We provide an algorithm to solve this problem in the chapter dedicated to CRN. The solution for relay selection is fairly similar to the one proposed for wireless relaying network. We provide numerical simulations comparing the performance of PSR and TSR protocols for various operating parameters.

1.3 Organization of the Thesis

This thesis consists of the following chapters:

Chapter 1: In the chapter, we explain the concept of wireless energy transfer and list out its applications. Then we compare various WET techniques and provide justification for choosing RF WET. Next comes the background information regarding the system model, problem overview, and our contributions.

Chapter 2: In this chapter, we give a surface-level explanation of the topics required to understand SWIET. These topics include the modes of WET, RF Energy Harvesting, and practical receiver architectures for SWIET. We also provide a circuit layout for the device used to convert RF to DC.

Chapter 3: We consider a WCRN, in which the relays are capable of performing SWIET. To facilitate SWIET at the relays, we propose two relaying protocols: TSR and PSR. The resource allocation and relay selection in this network is done according to the rate maximization problem.

Chapter 4: To address the concerns regarding spectrum efficiency put forward in the literature, we consider cooperative CRN in this chapter. The reader can find solutions for the rate maximization problem and numerical simulations that detail the performance of the relaying protocols.

Chapter 5: Provides brief introduction to our future interests.

Chapter 6: Concludes this work.

Chapter *2*

Wireless Energy Transfer

Simultaneous wireless energy and information transfer in a cooperative relaying network can achieve broad connectivity and energy efficiency at the same time. To understand SWIET, the knowledge of the latest trends in WET is necessary. In this chapter, we present various WET technologies with emphasis on RF energy transfer. A compact and efficient architecture to convert RF signals to DC is also studied. The shortcomings of the traditional receivers while handling SWIET are listed and then we present the measures taken by modern receivers to avoid these pitfalls.

2.1 Wireless Energy Transfer

Wireless energy transfer (WET) is the technique which transfers energy from a source to destination without the aid of interconnecting wires. The early developments in this field date back to the 19th century. In 1831, Michael Faraday introduced the principle of magnetic induction and during the same period, Maxwell formulated the laws that govern the behavior of EM radiation. Around 1899, Nikola Tesla successfully demonstrated WET by lighting several lamps from a distance. The current generation of wireless networks aims to tackle sophisticated issues like connection density, data rates, spectrum efficiency, e.t.c. The network topologies designed to address these issues often involve a multitude of devices performing an array of functions and they have immense energy demands. People began to see that integrating WET in a wireless network can be a clean and efficient way to meet this energy demand. Advances in the field of WET center chiefly on two classes, viz, near-field and far-field.

2.1.1 Near-Field WET

Near-field or non-radiative WET use techniques like inductive coupling, capacitive coupling, e.t.c, to transfer energy efficiently over a small distance. In this section, we discuss the merits and limitations of various near-field WET techniques and list out their applications.

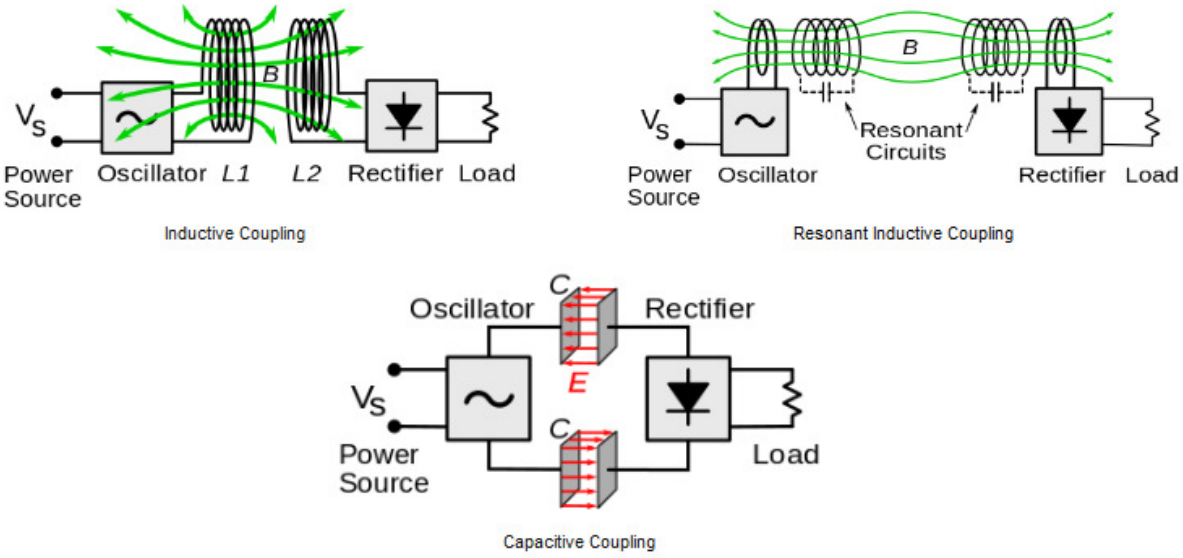

Figure 2.1 Near Field Techniques

2.1.1.1 Inductive Coupling

In inductive coupling, energy transfer takes place between coils by means of a magnetic field. The coil connected to the source generates a magnetic field, and this field induces an alternating voltage (EMF) at the terminals of the coil at the receiver. This EMF acts as a source for the alternating current (AC) at the receiver. We can pass this AC through a rectifier to convert it into direct current (DC), and use it to drive the load. According to Faraday's law of induction, the EMF generated at the receiver coil is directly proportional to the amount of flux passing through it. To ensure optimal energy transfer the source and the receiver coils should be close to each other so that most of the flux passes through the receiver coil. Inductive coupling WET has found it's usage in the cordless toothbrushes, smart access cards, and biomedical devices implanted in the body.

2.1.1.2 Resonant Circuits

Inductive coupling can transfer effectively over short distances. However, the efficiency of inductive WET drops drastically if the transmission range increases. With resonant inductive coupling (RIC), the range of WET can increase by using two coils which are tuned to resonate to the same frequency. The advantages of RIC over inductive coupling include greater range, high frequency of operation, and less EM interference [14].

2.1.1.3 Capacitive Coupling

In inductive coupling energy transferred between two inductors by a magnetic field [15]. In a similar fashion, one can use an electric field to transport energy. A pair of electrodes, one attached to an

AC source and another connected to the receiver form a capacitor. The electrode attached to the source generates an electric field which induces electrostatic potential at the receiver side electrode. The amount of energy transferred is directly proportional to the capacitance, which in turn decreases with the increase in the separation between the electrodes. Therefore, capacitive coupling is used to transport energy over short distances (up to one meter).

2.1.2 Far-Field WET

Far-field or radiative WET techniques employ radiation to transfer energy from source to receiver. Unlike near-field techniques, with far-field WET, one can transport energy over longer distances, typically in the range of kilometers [16]. RF waves and lasers are the most common forms of radiation used in this mode of WET. The directional nature of the lasers can guarantee efficient transfer, but, the photovoltaic cells used to convert the laser light to electric energy have less efficiency (40%-50%). Also, when used in high power applications the laser radiation can cause harm to the living things in the surroundings. RF signals can support SWIET, with potential to support the nodes located in remote regions. The devices used for transforming RF to electric energy, called rectenna, can achieve efficiency over 90%. By far WET using RF signals is the most popular choice among the far-field techniques. We dedicate the following section to discuss the basics of RF EH and present an architecture for the rectenna.

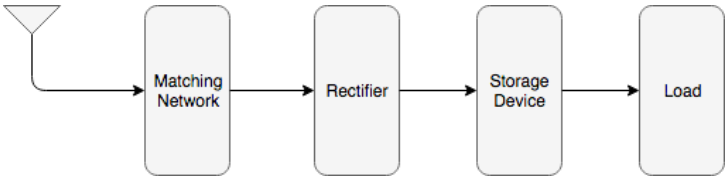

Figure 2.2 RF EH module

2.2 RF Energy Harvesting

With the increasing focus on Internet of things (IoT), and wireless sensor networks (WSN), EH using RF signals has received a lot of attention. EH is a technique in which the wireless devices harvest and store the ambient energy available in the surroundings. Nature has a wide array of sources like solar, wind, thermal e.t.c to choose for EH [17]. Unlike the conventional sources, RF EH can provide a reliable supply of energy, as they are less susceptible to the changes in the environment. Also, WET using RF waves is a far-field technique, so it can supply energy to devices located in remote regions. This feature is particularly useful in a network like WSN, which is made up of a large number of sensors distributed over a wide area. However, the strength of the signal can reduce due to the unwanted scattering of the rays by the particles present in the environment. We can combat this by carefully designing and

positioning the antennas to beamform the signal in the direction of the receiver. In [18], the authors propose a dynamic beamforming technique that uses multiple transmit and receive antennas to focus the signal, to achieve better energy transfer efficiency. The wireless devices generally receive their power from sources like batteries, which means their internal circuits are designed to run on DC voltage. Therefore, the wireless devices capable of EH should contain an additional unit that converts the RF signals to DC voltage. In this section, we provide a brief discussion of various stages involved in the conversion of RF to DC hoping that this helps to digest/accept the SWIET techniques presented in the following chapters.

2.2.1 Circuit Layout

The RF EH circuit consists of an antenna, a matching network, a rectifier, and storage devices like batteries as shown in Figure 2.2. The antenna collects the RF signal and converts it into AC voltage. The matching network does the impedance matching, to maximize the power delivered to the rectifier. The rectifier converts the output obtained at the terminals of the matching network to DC and stores the energy in a storage device [19]. The amount of RF energy present in the environment is limited, so, RF EH can only serve devices which can operate in the range of μW to mW [20]. The major design challenge is to make this module compact to suit the mobile nodes and enable it to function efficiently with the scantily available ambient energy. In [21], the authors use a microstrip patch antenna which is compact, has low cost, and pretty simple to manufacture. A Schottky diode with a proper threshold voltage can effectively rectify low amplitude AC signals [22].

2.3 SWIET

The scarcity of energy resources limits the performance of a network. SWIET has been proposed as a solution to meet the energy requirements of a network. In SWIET, we use RF waves to transmit information and energy using the same signal. The energy constrained nodes can harvest energy from the received signal and store it for further use. In [15], the authors investigate the challenges involved in integrating SWIET into various emerging wireless technologies. Since the signals employed in SWIET carry both information and energy, sophisticated receiver architectures are needed to make the operation of the network seamless. In the beginning, the receiver architectures proposed to support SWIET, assumed to perform energy harvesting and information decoding at the same time. However, the current hardware cannot achieve this in practice, without tampering the information content of the signal. Therefore, the practical receiver architectures try to separate the process of energy harvesting from information decoding. Some architectures achieve this by splitting the received signal, while others use separate antennas for energy harvesting and information decoding. In this section, we provide a brief survey on various practical receiver architectures studied in the literature.

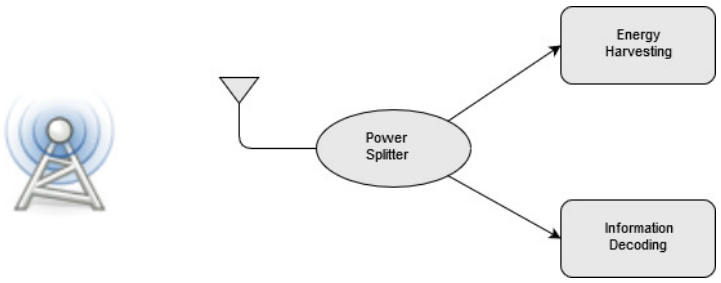

Figure 2.3 Power-Splitting Receiver Architecture

2.3.1 Power-Splitting Receiver

In this receiver architecture, at the receiver antenna, the received signal is split into two streams of different power levels. One stream is sent to the EH unit to extract the energy, while the other one is used to perform information decoding. We illustrate this procedure in Figure 5.5. Let ρ denote the power splitting (PS) ratio, which represents the ratio in which the power splitter segments the received signal. If r represents the received signal, then $\sqrt{\rho}r$ is used for EH and $\sqrt{(1-\rho)}r$ is used for ID. Let $P_{EH}(\rho)$ denote the total harvested power then it can be expressed as

$$P_{EH}(\rho) = \rho\eta\mathbb{E}\{|r|^2\}. \tag{2.1}$$

The parameter η in (2.1) represents the efficiency with which we can convert the harvested RF energy to DC. A method to obtain the optimal PS ratio for SISO and MIMO networks is studied exhaustively in [23].

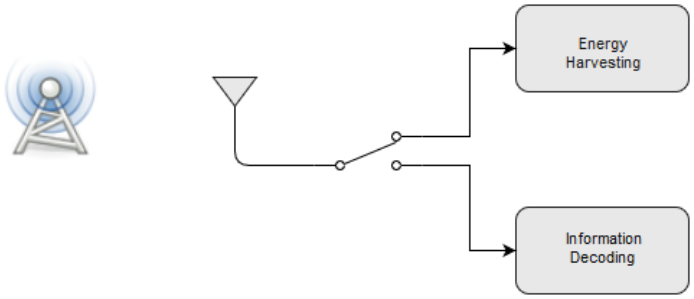

Figure 2.4 Time Switching Receiver Architecture

2.3.2 Time-Switching Receiver

Figure 2.4 displays the schematic of this receiver architecture. It mainly consists of two blocks, one for EH, and another for ID. The receiver harvests energy for a fraction of the time, and for the remaining time, it switches to ID. Let T denote the time period of communication, then as per the widely used convention, the receiver harvests for a period of αT, and decodes for a period of $(1-\alpha)$T. Here α is

known as the time-switching (TS) ratio and it lies in the range of (0,1). Let r represent the received signal then the total harvested power ($P_{EH}(\alpha)$) can be expressed as

$$P_{EH}(\alpha) = \alpha\eta\mathbb{E}\{|r|^2\}. \tag{2.2}$$

This receiver architecture is popular among the works that deal with SWIET [24, 25].

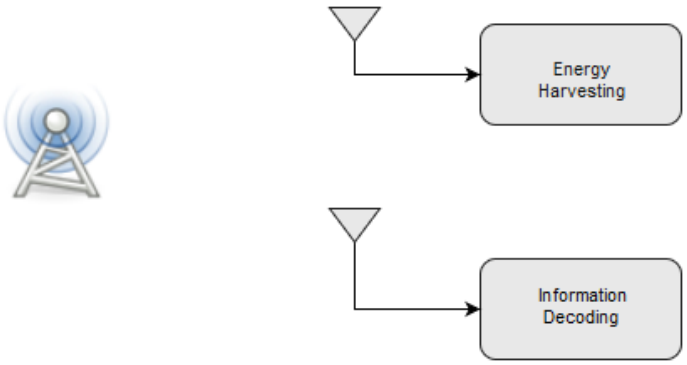

Figure 2.5 Separate Receiver Architecture

2.3.3 Separate Receiver

This receiver consists of an EH unit and an ID unit, deployed as separate receivers . They receive the signal from the same source and carry out their respective functions independently. The separation of EH and ID units provide the flexibility to implement different designs without affecting the performance of each other. We can study the channel state information (CSI) and provide feedback to the transmitter to optimize the trade-off between the achievable information rate and the harvested energy [26].

2.3.4 Antenna Switching Receiver

To implement TS receiver in practice, one should dedicate a lot of resources to achieve and maintain proper time synchronization. In the case of PS receiver architecture also, the performance may be low due to imperfections in the underlying hardware [26]. The antenna switching receiver architecture is pretty simple to implement in practice, as it involves a simple antenna switching between EH and ID to achieve SWIET. For example, a sub-group (L) from the total number of receiver antennas (N_R) can perform EH, and the rest (N_R-L) can take part in ID. In Figure 2.6, the receiver has two antennas we use one for EH and another for ID.

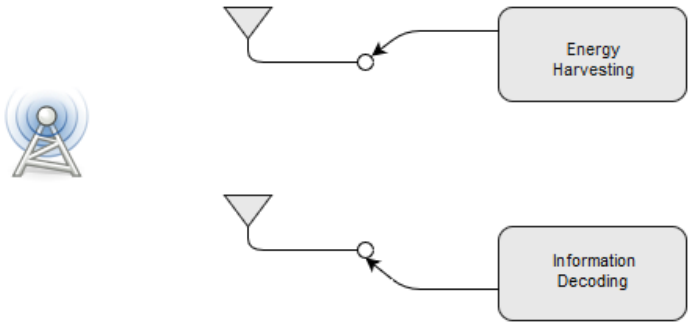

Figure 2.6 Antenna Switching Receiver Architecture

2.4 Summary

Generally, in SWIET, a transmitter sends a signal that carries both energy and information and the receiver harvests the energy and forwards the signal for further processing. To understand how one achieves this in practice, the reader should know about WET, and the techniques the receivers use to handle SWIET. In this chapter, we provided a brief overview of the concepts required to understand the various stages involved in achieving SWIET.

Chapter *3*

Simultaneous Wireless Information and Energy Transfer in Cooperative Networks

In a wireless sensor network (WSN) the sensor nodes are often distributed in different geographical locations. This limits the range of direct communication between the sensor nodes and brings down the overall network connectivity. The connectivity issue is not limited to a WSN; it is prevalent in most of the emerging wireless networks. People started to use intermediate devices called relays to aid the communication between these estranged nodes. The relays need to expend some energy to carry out this process and if the relays themselves are energy constrained this added expenditure is not desired. A relay capable of EH can sustain itself without any external energy source and thus improves the network connectivity.

In this chapter, we introduce SWIET in a wireless cooperative relaying network. We propose the TSR and PSR protocols to facilitate energy harvesting and information processing at the relay. For the TSR and PSR protocols, we derive expressions for the achievable signal to noise interference ratio (SINR) at the destination and address the problem of optimal resource allocation and relay selection to maximize the rate of communication between the transceiver nodes. For both protocols, we propose an optimal scheme for power allocation along with energy harvesting and optimal relay selection. In both the cases, we arrive at a mixed-integer programming optimization problem. This is simplified using high SINR approximation of the instantaneous sum-rate to obtain closed form solutions.

The chapter is organized as follows. Introduction to the current state of the art is provided in section 3.1. Section 3.2 gives an overview of the system model. Section 3.3 describes the PSR protocol and section 3.4 describes the TSR protocol. In Section 3.5, we address optimal resource allocation and relay selection problem. Finally, section 3.5 provides the summary of this chapter.

3.1 Introduction

A network can have access to a continuous supply of energy by harvesting energy from its surroundings. Energy harvesting from radio-frequency (RF) signals has received great attention recently [2], [1],

[3]. RF signals can carry both energy and information at the same time, enabling communication node to harvest energy and extract information simultaneously. In [1], the authors propose capacity-energy function to outline the fundamental tradeoffs in simultaneous information and energy transfer. In [2], the work in [1] is extended to frequency-selective channels with additive white Gaussian noise (AWGN).

Recent advances in simultaneous information transfer and energy harvesting using RF signals generally follow two approaches. In the first approach, the same receiver is able to process the information as well as extract energy from the received signal [1, 2]. This receiver architecture may not hold in practice [3], as circuits used for harvesting energy from RF signals are not yet able to decode the carried information directly. As discussed in the previous chapter, the second approach considers practical receiver architectures, namely, TS and PS, proposed in [27, 4, 5]. Cooperative relay techniques have been employed in wireless networks to achieve better network connectivity, efficient utilization of resources such as power and bandwidth. In the context of simultaneous transfer of energy and information, TS-based relaying (TSR) and PS-based relaying (PSR) can be employed in the cooperative systems [10], [11].

3.2 System Model

We consider a wireless co-operative network consisting of two transceiver nodes, T_1 and T_2, and a set of two-way relays. The transceivers communicate with each other via a relay node selected from a set of L two-way relay nodes. We assume that there is no direct line between T_1 and T_2. The two-way relay harvests energy from the RF signals broadcasted by the transceiver nodes and uses the harvested energy to amplify and forward the signals to their destination. All the nodes are equipped with a single antenna. Based on the time switching and the power splitting receiver architectures, we propose two relaying protocols to harvest energy from the RF signal, (i) PSR protocol and (ii) TSR protocol. We provide detailed analysis of the PSR and TSR protocols in the following sections.

3.3 PSR Protocol

As shown in Fig 3.2, communication between the transceiver nodes in PSR protocol takes place over two time slots. In the first slot, the transmission of signal takes place at both transceiver nodes. The transmitted signals are then received by the relay. Let $x_1 \in \mathbb{C}$ and $x_2 \in \mathbb{C}$ be the transmit signals conveyed by the two transceiver nodes T_1 and T_2, respectively. We assume that $\mathbb{E}\{|x_1|^2\} = \mathbb{E}\{|x_2|^2\} = 1$, where $\mathbb{E}\{\cdot\}$ is the expectation operator and $|\cdot|$ denotes absolute value. The signal received by the ith relay, denoted by r_i, can be expressed as

$$r_i = \sqrt{P_1} h_i x_1 + \sqrt{P_2} g_i x_2 + \delta_i, \quad 1 \leq i \leq L, \tag{3.1}$$

where P_1 and P_2 are the transmit powers of T_1 and T_2 respectively, h_i denotes the channel gain from T_1 to the ith relay, g_i denotes the channel gain from T_2 to the ith relay and $\delta_i \sim \mathcal{CN}(0, \sigma_{\delta_i}^2)$ is the additive

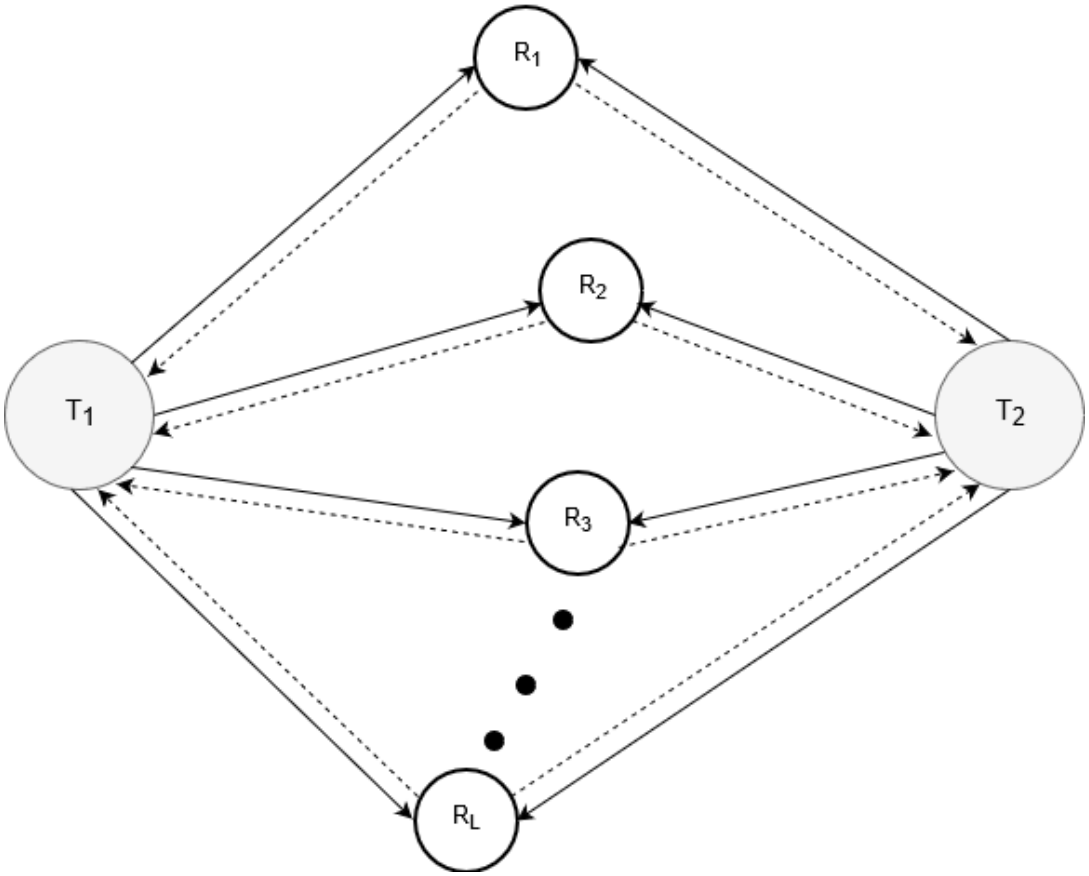

Figure 3.1 Wireless Cooperative Relaying Network

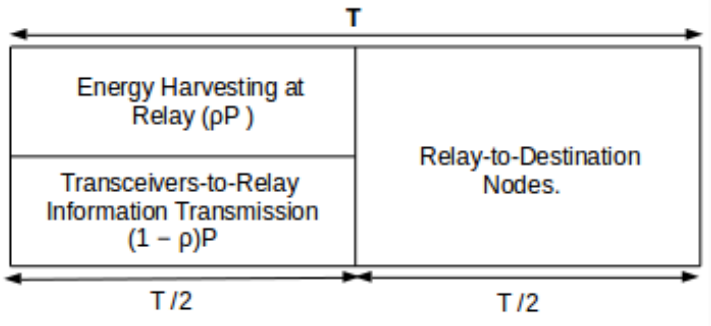

Figure 3.2 Structure of PSR time-block

white Gaussian noise (AWGN) at the ith relay. In the second slot, the signal received by the ith relay, r_i is split into two parts for energy harvesting and information processing. Let $\rho \in [0, 1]$ be the power splitting ratio, meaning that $\sqrt{\rho}r_i$ is used for energy harvesting and $\sqrt{(1-\rho)}r_i$ is used for information processing. The total energy harvested at the ith relay, denoted by $P_{EH}(\rho)$, can be expressed as

$$P_{EH}(\rho) = \rho\eta\mathbb{E}\{|r_i|^2\} \tag{3.2}$$

$$= \rho\eta[P_1|h_i|^2 + P_2|g_i|^2 + \sigma_{\delta_i}^2], \tag{3.3}$$

where $\eta \in [0, 1]$ denotes the energy conversion efficiency. The remaining fraction of the received signal, $\sqrt{1-\rho}r_i$, is retransmitted by the relay after amplifying it by a complex number. Both the transceiver nodes receive the signal transmitted by the relay node. The signal received by the transceiver T_1 can be written as

$$y_1 = \sqrt{1-\rho}[\sqrt{P_1}w_i h_i h_i x_1 + \sqrt{P_2}w_i g_i h_i x_2 + w_i h_i \delta_i] + \phi_1, \tag{3.4}$$

where $w_i \in \mathbb{C}$ is the amplification factor or weight coefficient of the ith relay, ϕ_1 represents the AWGN at transceiver T_1 with zero mean and variance $\sigma_{\phi_1}^2$. The signal received by the transceiver T_2 is given by

$$y_2 = \sqrt{1-\rho}[\sqrt{P_1}w_i h_i g_i x_1 + \sqrt{P_2}w_i g_i g_i x_2 + w_i g_i \delta_i] + \phi_2, \tag{3.5}$$

where ϕ_2 represents the AWGN at transceiver T_2 with zero mean and variance $\sigma_{\phi_2}^2$. The terms $\sqrt{P_1}w_i h_i h_i x_1$ and $\sqrt{P_2}w_i g_i g_i x_2$ in (3.4) and (3.5), respectively, represent the self-interference terms resulting from both transceivers own transmitted signals. The self-interference terms can be eliminated from the received signals using the knowledge of the channel state information (CSI), the amplification factor and each transceiver's transmitted signal. The SINR at transceiver T_1 after self-interference cancellation is given by

$$SINR_{i,1} = \frac{(1-\rho)P_2|w_i|^2|h_i|^2|g_i|^2}{(1-\rho)\sigma_{\delta_i}^2|w_i|^2|h_i|^2 + \sigma_{\Phi_1}^2}, \tag{3.6}$$

and the SINR at transceiver T_2 is given by

$$SINR_{i,2} = \frac{(1-\rho)P_1|w_i|^2|h_i|^2|g_i|^2}{(1-\rho)\sigma_{\delta_i}^2|w_i|^2|g_i|^2 + \sigma_{\Phi_2}^2}. \tag{3.7}$$

The transmit power of the ith relay can be expressed as

$$P_{Ri} = \mathbb{E}\{|w_i\sqrt{1-\rho}r_i|^2\} \tag{3.8}$$

$$= (1-\rho)[P_1|w_i|^2|h_i|^2 + P_2|w_i|^2|g_i|^2 + |w_i|^2\sigma_{\delta_i}^2], \tag{3.9}$$

from (3.9), we have

$$|w_i| = \frac{\sqrt{P_{Ri}}}{\sqrt{(1-\rho)[P_1|h_i|^2 + P_2|g_i|^2 + \sigma_{\delta_i}^2]}}. \tag{3.10}$$

Along the same lines, we can express the the SINR at the transceivers T_1 and T_2 in terms of P_{Ri} as follows:

$$SINR_{1,i} = \frac{P_2 P_{Ri}|h_i|^2|g_i|^2}{P_{Ri}\sigma_{\delta_i}^2|h_i|^2 + \sigma_{\Phi_1}^2(P_1|h_i|^2 + P_2|g_i|^2 + \sigma_{\delta_i}^2)}, \tag{3.11}$$

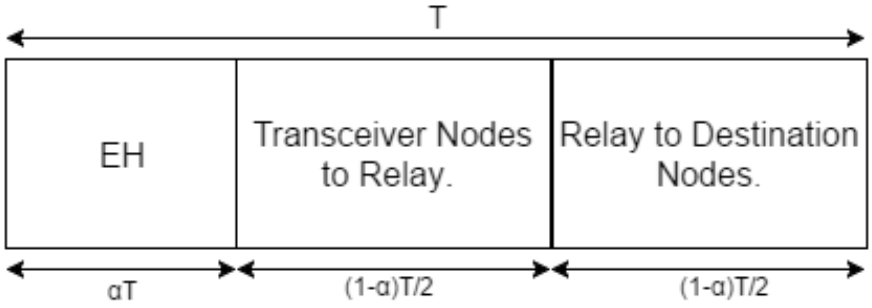

Figure 3.3 Transmission time-block structure for TSR protocol

$$SINR_{2,i} = \frac{P_1 P_{Ri} |h_i|^2 |g_i|^2}{P_{Ri}\sigma_{\delta_i}^2 |g_i|^2 + \sigma_{\Phi_2}^2 (P_1 |h_i|^2 + P_2 |g_i|^2 + \sigma_{\delta_i}^2)}. \tag{3.12}$$

3.4 TSR Protocol

Let us denote the total time of transmission block by T. In TS, the receiver does EH for a fraction of the transmission time and does information processing for the remaining time. Let $\alpha \mathrm{T}$ denote the EH phase, and $(1-\alpha)\mathrm{T}$ represents the information processing phase. Here, α is called the time switching ratio, and it lies in the range of $0 \leq \alpha \leq 1$. The information processing phase consists of two parts: transceiver to relay transmission takes place in the first half, and in the latter half the relay transmits the signal to the destination. This procedure is illustrated in Fig. 3.3. Let $x_1 \in \mathbb{C}$ and $x_2 \in \mathbb{C}$ be the transmit signals conveyed by the two transceiver nodes T_1 and T_2, respectively. We assume that $\mathbb{E}\{|x_1|^2\} = \mathbb{E}\{|x_2|^2\} = 1$. The signal received by the ith relay, denoted by r_i, can be expressed as

$$r_i = \sqrt{P_1} h_i x_1 + \sqrt{P_2} g_i x_2 + \delta_i, \quad 1 \leq i \leq L, \tag{3.13}$$

Energy is harvested from the received signal for a duration of $\alpha \mathrm{T}$, and the harvested energy at relay node can be expressed as

$$P_{EH}(\alpha) = \alpha\eta \mathbb{E}\{|r_i|^2\} \tag{3.14}$$

$$= \alpha\eta [P_1 |h_i|^2 + P_2 |g_i|^2 + \sigma_{\delta_i}^2], \tag{3.15}$$

where $\eta \in [0, 1]$ is the energy conversion efficiency of the energy harvesting receiver.

During the information receiving phase, the received signal is the same as (3.13), but received in a different time duration. The signal received by the relay is re-transmitted after amplifying it by a complex number. Both the transceiver nodes receive the signal transmitted by the relay node. The signal received by the transceiver T_1 can be written as

$$y_1 = [\sqrt{P_1} w_i h_i h_i x_1 + \sqrt{P_2} w_i g_i h_i x_2 + w_i h_i \delta_i] + \phi_1, \tag{3.16}$$

where $w_i \in \mathbb{C}$ is the amplification factor or weight coefficient of the ith relay, ϕ_1 represents the AWGN at transceiver T_1 with zero mean and variance $\sigma^2_{\phi_1}$. The signal received by the transceiver T_2 is given by

$$y_2 = [\sqrt{P_1} w_i h_i g_i x_1 + \sqrt{P_2} w_i g_i g_i x_2 + w_i g_i \delta_i] + \phi_2, \tag{3.17}$$

The terms $\sqrt{P_1} w_i h_i h_i x_1$ and $\sqrt{P_2} w_i g_i g_i x_2$ in (3.16) and (3.17), respectively, represent the self-interference terms resulting from both transceivers' own transmitted signals. The SINR at transceiver T_1 after self-interference cancellation is given by

$$SINR_{i,1} = \frac{P_2 |w_i|^2 |h_i|^2 |g_i|^2}{\sigma^2_{\delta_i} |w_i|^2 |h_i|^2 + \sigma^2_{\Phi_1}}, \tag{3.18}$$

and the SINR at transceiver T_2 is given by

$$SINR_{i,2} = \frac{P_1 |w_i|^2 |h_i|^2 |g_i|^2}{\sigma^2_{\delta_i} |w_i|^2 |g_i|^2 + \sigma^2_{\Phi_2}}. \tag{3.19}$$

The transmit power of the ith relay can be expressed as

$$P_{Ri} = \mathbb{E}\{|w_i r_i|^2\} \tag{3.20}$$

$$= P_1 |w_i|^2 |h_i|^2 + P_2 |w_i|^2 |g_i|^2 + |w_i|^2 \sigma^2_{\delta_i}, \tag{3.21}$$

from (3.21), we have

$$|w_i| = \frac{\sqrt{P_{Ri}}}{P_1 |h_i|^2 + P_2 |g_i|^2 + \sigma^2_{\delta_i}}. \tag{3.22}$$

Along the same lines, we can express the the SINR at the transceivers T_1 and T_2 in terms of P_{Ri} as follows:

$$SINR_{1,i} = \frac{P_2 P_{Ri} |h_i|^2 |g_i|^2}{P_{Ri} \sigma^2_{\delta_i} |h_i|^2 + \sigma^2_{\Phi_1} (P_1 |h_i|^2 + P_2 |g_i|^2 + \sigma^2_{\delta_i})}, \tag{3.23}$$

$$SINR_{2,i} = \frac{P_1 P_{Ri} |h_i|^2 |g_i|^2}{P_{Ri} \sigma^2_{\delta_i} |g_i|^2 + \sigma^2_{\Phi_2} (P_1 |h_i|^2 + P_2 |g_i|^2 + \sigma^2_{\delta_i})}. \tag{3.24}$$

3.5 Optimal Relay Selection and Power Allocation

The objective of the problem is to maximize the overall rate under energy-harvesting and transmit power constraints. This objective is achieved by choosing the best relay, which operates with the energy provided by the transceivers, and by optimal resource allocation at the transceivers and the relay node. This problem can be formulated as

$$\max_{k \in \mathcal{I}, (P_1, P_2, P_{R_k}, \xi) \in \Lambda} \quad R_k, \tag{3.25}$$

where R_k is the achievable rate when the kth relay is operating, and $\mathcal{I}$ is the set of relay indices. The feasible set Λ is defined by the power and energy harvesting constraints. This is a joint optimization

over the relay indices, the transmit powers, and the variable ξ. ξ represents ρ in case of PSR and α in case of TSR. As such it is a mixed-integer program and hard to solve. However, since only one relay will be operating at any given time, this optimization can be performed in two simple steps; first over the transmit powers and the variable ξ and then over the relay indices, as given below:

$$\max_{k\in 1,2,\ldots,L} \quad \max_{P_1,P_2,P_{R_k},\xi \epsilon\ \Lambda} \quad R_k. \tag{3.26}$$

Consequently, first we maximize the rate with respect to the variable ξ and transceiver transmit powers. We consider the resource allocation problem, in PSR and TSR protocols, in the following sections.

3.5.1 Resource Allocation in PSR Protocol

The instantaneous achievable rate of the wireless co-operative network with two-way relaying is given as

$$R_i = \frac{1}{2}\log(1+SINR_{i,1}) + \frac{1}{2}\log(1+SINR_{i,2}). \tag{3.27}$$

The factor of $\frac{1}{2}$ used in (3.27), results from the two time slots required to complete the information exchange between the transceivers. In order to make the mathematical analysis more viable, we follow the following high-SINR approximation of the rate:

$$\begin{aligned} R_i &\approx \frac{1}{2}\log\left(\frac{P_2 P_{Ri}|h_i|^2|g_i|^2}{P_{Ri}\sigma_{\delta_i}^2|h_i|^2 + \sigma_{\Phi_1}^2(P_1|h_i|^2 + P_2|g_i|^2 + \sigma_{\delta_i}^2)}\right) \\ &+ \frac{1}{2}\log\left(\frac{P_1 P_{Ri}|h_i|^2|g_i|^2}{P_{Ri}\sigma_{\delta_i}^2|g_i|^2 + \sigma_{\Phi_2}^2(P_1|h_i|^2 + P_2|g_i|^2 + \sigma_{\delta_i}^2)}\right) \\ &= \frac{1}{2}\log\left(\frac{P_1 P_2 P_{R_i}^2|h_i|^4|g_i|^4}{X_i Y_i}\right), \end{aligned} \tag{3.28}$$

where

$$X_i = P_{Ri}\sigma_{\delta_i}^2|h_i|^2 + \sigma_{\Phi_1}^2(P_1|h_i|^2 + P_2|g_i|^2 + \sigma_{\delta_i}^2), \tag{3.29}$$

$$Y_i = P_{Ri}\sigma_{\delta_i}^2|g_i|^2 + \sigma_{\Phi_2}^2(P_1|h_i|^2 + P_2|g_i|^2 + \sigma_{\delta_i}^2). \tag{3.30}$$

This high SINR approximation can significantly simplify the optimal power allocation and PS ratio computation, which can now be reformulated as

$$\begin{aligned} \max_{P_1,P_2,P_{Ri},\rho} \quad & \frac{1}{2}\log\left(\frac{P_1 P_2 P_{Ri}^2|h_i|^4|g_i|^4}{X_i Y_i}\right) \\ \text{s.t.} \quad & P_1 + P_2 \le P_T, \\ & P_{EH}(\rho) \ge \theta, \\ & P_{Ri} \le \theta, \\ & 0 \le \rho \le 1, \end{aligned} \tag{3.31}$$

where P_T is the total transmit power of the two transceiver nodes T_1 and T_2 and θ is the minimum amount of the energy harvested at the relay. Note that θ is also the upper limit for the transmit power at the relay, meaning that the relay uses only the harvested energy to amplify and retransmit the received signal. The transmit power constraint and energy harvesting constraint acts as a safeguard such that the transmit power at the relay does not exceed the harvested power. As the objective function of (3.31) is a monotonically increasing function of the transmit power of *i*th relay, P_{Ri}, it is self-evident that its optimal value is given by $P'_{Ri} = \theta$. Having realized the optimal value of P_{Ri}, we proceed to compute the optimal value of (P_1, P_2, ρ). Then, the problem in (3.31) can be stated as follows:

$$\begin{aligned} \max_{P_1,P_2,\rho} \quad & \frac{1}{2}\log\left(\frac{P_1 P_2 {P^*_{Ri}}^2 |h_i|^4 |g_i|^4}{X'_i Y'_i}\right) \\ \text{s.t.} \quad & P_1 + P_2 \leq P_T, \\ & P_{EH} \geq \theta, \\ & 0 \leq \rho \leq 1, \end{aligned} \tag{3.32}$$

where X'_i and Y'_i are obtained from X_i and Y_i, respectively, by replacing P_{Ri} with P'_{Ri} in (3.29) and (3.30). Since the logarithmic function is a monotonically increasing function, the maximization in (3.32) is equivalent to the minimization problem as follows:

$$\begin{aligned} \min_{P_1,P_2,\rho} \quad & \frac{X'_i Y'_i}{P_1 P_2 P'_{Ri} |h_i|^4 |g_i|^4} \\ \text{s.t.} \quad & P_1 + P_2 \leq P_T, \\ & P_{EH} \geq \theta, \\ & 0 \leq \rho \leq 1. \end{aligned} \tag{3.33}$$

We describe two solutions to this problem; optimal and a low-complexity suboptimal solution. Both of the proposed solutions have closed form.

3.5.1.1 Optimal Scheme

We obtain optimal power allocation and power splitting ratio using the Karush-Kuhn-Tucker conditions. In order to facilitate further analysis, we rewrite (3.33) as follows:

$$\begin{aligned} \min_{P_1,P_2,\rho} \quad & \frac{(a_1 + b_1 P_1 + c_1 P_2)(a_2 + b_2 P_1 + c_2 P_2)}{P_1 P_2} \\ \text{s.t.} \quad & P_1 + P_2 \leq P_T, \\ & \rho(m P_1 + n P_2 + q) \geq \theta, \\ & 0 \leq \rho \leq 1, \end{aligned} \tag{3.34}$$

where

$$a_1 = \frac{\sigma_{\pi_i}^2}{P_{Ri}^*|g_i|^2}\left[1+\frac{\sigma_{\Phi_1}^2}{|h_i|^2}\right], \quad a_2 = \frac{\sigma_{\pi_i}^2}{P_{Ri}^*|h_i|^2}\left[1+\frac{\sigma^2\Phi_2}{|g_i|^2}\right], b_1 \quad = \frac{\sigma_{\Phi_1}^2}{P_{Ri}^*|g_i|^2}, \quad b_2 = \frac{\sigma_{\Phi_2}^2}{P_{Ri}^*|g_i|^2}, \quad c_1 = \frac{\sigma_{\Phi_1}^2}{P_{Ri}^*|h_i|^2},$$

$$c_2 = \frac{\sigma_{\Phi_2}^2}{P_{Ri}^*|h_i|^2}, \quad m = \eta|h_i|^2, \quad n = \eta|g_i|^2, \text{ and } q = \eta\sigma_{\pi_i}^2.$$

Then, the Lagrangian associated with the problem in (3.34) is given by

$$\mathcal{L}(P_1, P_2, \rho, \mu) = f + \mu_1[\theta - \rho(mP_1 + nP_2 + q)] + \mu_2(P_1 + P_2 - P_T) + \mu_3(\rho - 1) - \mu_4\rho,$$

where $f = \frac{(a_1+b_1P_1+c_1P_2)(a_2+b_2P_1+c_2P_2)}{P_1P_2}$ and $\{\mu_i\}_{i=1}^4$ are the Lagrangian multipliers. The optimal solution satisfies the following KKT conditions:

$$\frac{\partial f}{\partial P_1} - \mu_1\rho m + \mu_2 = 0, \frac{\partial f}{\partial P_2} - \mu_1\rho n + \mu_2 = 0, \mu_1[\theta - \rho(mP_1 + nP_2 + q)] = 0, \mu_2(P_1 + P_2 - P_T) = 0,$$
$$\mu_3(\rho - 1) = 0, \mu_4\rho = 0, \mu_i \geq 0, \ i = 1, 2, 3, 4,$$

By solving the set of KKT conditions given above, we obtain the optimal values of P_1, P_2, and ρ as follows:

$$P_1' = \frac{P_T\left[r_3\sqrt{1+\frac{r_1+r_2}{r_3}+\frac{r_1r_2}{r_3^2}} - (r_2+r_3)\right]}{r_1 - r_2}, \tag{3.35}$$

$$P_2' = \frac{P_T\left[(r_1+r_3) - r_3\sqrt{1+\frac{r_1+r_2}{r_3}+\frac{r_1r_2}{r_3^2}}\right]}{r_1 - r_2}, \tag{3.36}$$

$$\rho' = \frac{\theta}{\eta(P_1'|h_i^2| + P_2'|g_i|^2 + \sigma_{\pi_i}^2)}, \tag{3.37}$$

where $r_1 = b_1b_2 + \frac{a_1b_2}{P_T} + \frac{a_2b_1}{P_T}$, $r_2 = c_1c_2 + \frac{a_1c_2}{P_T} + \frac{a_2c_1}{P_T}$, and $r_3 = \frac{a_1a_2}{P_T^2}$.

3.5.1.2 Sub-Optimal Scheme

In the previous section, we considered a total transceiver power constraint to obtain the optimal solution. Here, we propose a simplified sub-optimal scheme for computing power allocation and power-splitting ratio. In this sub-optimal scheme, we consider a trivial power allocation such that $P_1 = P_2 = P$ and the problem in (3.33) is equivalent to follows:

$$\begin{aligned} \min_{P,\rho} \quad & \left(\frac{e_1}{P} + f_1\right)\left(\frac{e_2}{P} + f_2\right) \\ \text{s.t.} \quad & P \leq P_T/2, \\ & \eta\rho(P(|h_i^2| + |g_i|^2) + \sigma_{\pi_i}^2) \geq \theta, \\ & 0 \leq \rho \leq 1, \end{aligned} \tag{3.38}$$

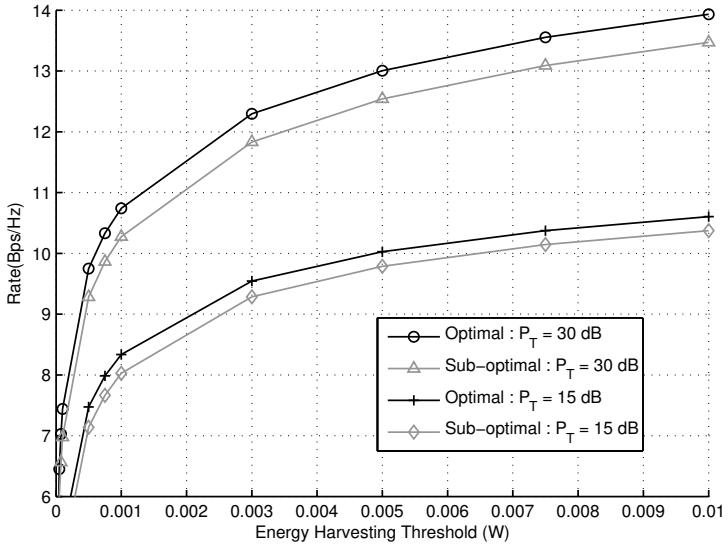

Figure 3.4 Rate versus energy harvesting threshold (θ) for different values of P_T

where $e_1 = P_{Ri}^* \sigma_{\pi_i}^2 |h_i|^2 + \sigma_{\pi_i}^2 \sigma_{\Phi_1}^2$, $e_2 = P_{Ri}^* \sigma_{\pi_i}^2 |g_i|^2 + \sigma_{\pi_i}^2 \sigma_{\Phi_2}^2$, $f_1 = \sigma_{\Phi_1}^2 (|h_1|^2 + |g_i|^2)$, and $f_2 = \sigma_{\Phi_2}^2 (|h_i|^2 + |g_i|^2)$. We can observe that the objective function in the problem given above is maximized when P takes the maximum value, i.e., $P = P_1' = P_2' = \frac{1}{2} P_T$, when $\rho' = \frac{2\theta}{\eta P_T (|h_i^2| + |g_i|^2)}$, then the minimum value of the objective function in (3.38) is given by $\left(\frac{2e_1}{P_T} + f_1\right)\left(\frac{2e_2}{P_T} + f_2\right)$.

3.5.1.3 Simulation Results

In this section, we illustrate the performance of the proposed joint relay selection and optimal power allocation scheme with energy harvesting through simulations. Precisely, we evaluate the performance of the optimal scheme with that of the sub-optimal scheme. We assume that all the channels undergo Rayleigh fading.

Firstly, we study the performance of the proposed schemes in terms of maximum achievable rate versus energy harvesting threshold. The corresponding results are provided for total transmit power limits of $P_T = 15$ dB and $P_T = 30$ dB. The energy harvesting threshold (θ) ranges from 1 mJ to 10 mJ. The performance results are displayed in Fig. 3.4. We can observe that the proposed optimal scheme outperforms the sub-optimal uniform power allocation scheme. The rates obtained in Fig. 1 are high, thus validating the high-SINR approximation used above.

Secondly, we demonstrate the performance of the proposed schemes in terms of the rate versus total transmitted power of the transceivers. The energy harvesting threshold (θ) used in this experiment are 0 dBm, 3 dBm , 8 dBm and 10 dBm. The total transmitted power P_T ranges from 0 dB to 30 dB. The performance results are displayed in Fig. 3.5. Here, as expected we can observe that the rates are increasing with increasing transmit power.

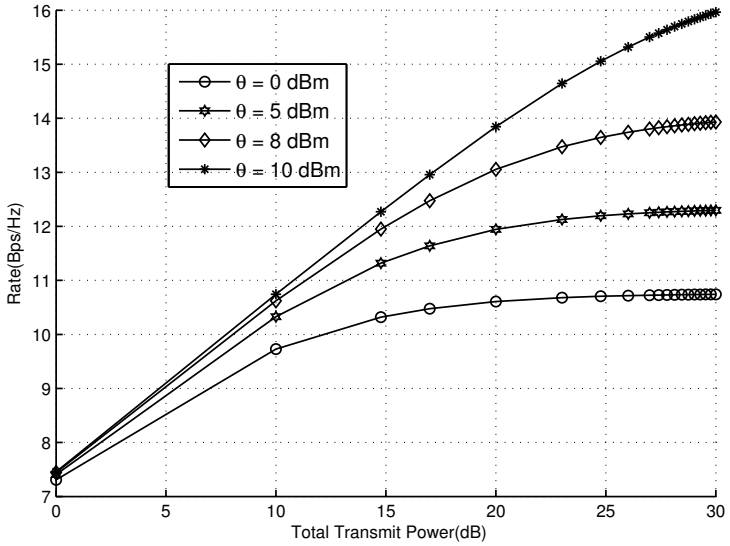

Figure 3.5 Rate versus total transmit power (P_T) for different values of θ

3.5.2 Resource allocation in TSR Protocol

The instantaneous achievable rate of the wireless co-operative network with two-way relaying is given as

$$R_i = \frac{1-\alpha}{2}\log(1+SINR_{i,1}) + \frac{1-\alpha}{2}\log(1+SINR_{i,2}). \tag{3.39}$$

The factor of $\frac{1-\alpha}{2}$ used in (3.39), results from the two time slots required to complete the information exchange between the transceivers. We follow the high-SINR approximation of the rate:

$$\begin{aligned} R_i &\approx \frac{1-\alpha}{2}\times \\ &\left\{\log\left(\frac{P_2 P_{Ri}|h_i|^2|g_i|^2}{P_{Ri}\sigma_{\delta_i}^2|h_i|^2+\sigma_{\Phi_1}^2(P_1|h_i|^2+P_2|g_i|^2+\sigma_{\delta_i}^2)}\right)\right. \\ &\left.+\log\left(\frac{P_1 P_{Ri}|h_i|^2|g_i|^2}{P_{Ri}\sigma_{\delta_i}^2|g_i|^2+\sigma_{\Phi_2}^2(P_1|h_i|^2+P_2|g_i|^2+\sigma_{\delta_i}^2)}\right)\right\} \\ &= \frac{1-\alpha}{2}\log\left(\frac{P_1 P_2 P_{R_i}^2|h_i|^4|g_i|^4}{X_i Y_i}\right), \end{aligned} \tag{3.40}$$

where

$$X_i = P_{Ri}\sigma_{\delta_i}^2|h_i|^2+\sigma_{\Phi_1}^2(P_1|h_i|^2+P_2|g_i|^2+\sigma_{\delta_i}^2), \tag{3.41}$$

$$Y_i = P_{Ri}\sigma_{\delta_i}^2|g_i|^2+\sigma_{\Phi_2}^2(P_1|h_i|^2+P_2|g_i|^2+\sigma_{\delta_i}^2). \tag{3.42}$$

As in the case of PSR protocol, we can use high SINR approximation to simplify the optimal power allocation and TS ratio computation, which can now be reformulated as

$$\begin{aligned} \max_{P_1,P_2,P_{Ri},\alpha} \quad & \frac{1-\alpha}{2}\log\left(\frac{P_1P_2P_{Ri}^2|h_i|^4|g_i|^4}{X_iY_i}\right) \\ \text{s.t.} \quad & P_1+P_2 \leq P_T, \\ & P_{EH} \geq \theta, \\ & P_{Ri} \leq \theta, \\ & 0 \leq \alpha \leq 1, \end{aligned} \tag{3.43}$$

where P_T is the total transmit power of the two transceiver nodes T_1 and T_2 and θ is the minimum amount of the energy harvested at the relay.

As the objective function of (3.43), is a monotonically increasing function of the transmit power of *i*th relay, P_{Ri}, it is self-evident that its optimal value is given by $P'_{Ri} = \theta$. Having realized the optimal value of P_{Ri}, we proceed to compute the optimal value of (P_1, P_2, α). Then, the problem in (3.43) can be stated as follows:

$$\begin{aligned} \max_{P_1,P_2,\alpha} \quad & \frac{1-\alpha}{2}\log\left(\frac{P_1P_2{P_{Ri}^*}^2|h_i|^4|g_i|^4}{X_i'Y_i'}\right) \\ \text{s.t.} \quad & P_1+P_2 \leq P_T, \\ & P_{EH} \geq \theta, \\ & 0 \leq \alpha \leq 1, \end{aligned} \tag{3.44}$$

We propose two solutions to this problem (3.44); optimal solution and a low complexity sub-optimal solution

3.5.2.1 Optimal Scheme

If α in (3.44) is a constant, we can solve this problem in the same lines as (3.32) . This involves formulating an equivalent minimization problem for (3.44), and solving this problem for a constant α. This procedure is carried out over the range of α, to select the value which maximizes the objective, and satisfies the energy harvesting threshold constraint. With $\alpha = 0$, the energy harvesting threshold of (3.44) cannot be satisfied for a nonzero value of θ. So, we initialize the linear search with a value of α close to zero.

Let us denote the objective of (3.44) by R, and R' represents the maximum value of this objective. P_1', P_2', and α' represents the optimal values corresponding to R'. The value of the increment δ can be chosen so as to ensure the required accuracy. Following the procedure illustrated below, we can arrive at P_1', P_2' and α', the optimal values of the rate maximization problem. The proposed solution can be outlined as follows:

Algorithm 1 Proposed Resource Allocation Algorithm

procedure OPTIMAL TSR
  Initialize α; θ; δ; $P_1' \leftarrow 0$; $P_2' \leftarrow 0$; $R' \leftarrow 0$.
  while $\alpha \leq 1$ **do**
    Solve (3.44) analogous to (3.38), obtain P_1 and P_2.
    Calculate R using P_1 and P_2.
    if $R \geq R'$ **then**
      set $\alpha' = \alpha$; $P_1' = P_1$; $P_2' = P_2$;$R' = R$.
      $\alpha = \alpha + \delta$.
    else
      $\alpha = \alpha + \delta$.
    end if
  end while
end procedure

3.5.2.2 Sub-Optimal Scheme

Here, we propose a simplified sub-optimal scheme for computing power allocation and time-splitting ratio. In this sub-optimal scheme, we simplify the resource allocation problem by allowing $P_1 = P_2 = P$, and the problem in (3.43) is equivalent to:

$$\begin{aligned} \max_{P,\alpha} \quad & \frac{1-\alpha}{2} \log \left(\frac{P^2 {P_{Ri}^*}^2 |h_i|^4 |g_i|^4}{\hat{X}_i' \hat{Y}_i'} \right) \\ \text{s.t.} \quad & P \leq P_T/2, \\ & \eta\alpha(P(|h_i^2| + |g_i|^2) + \sigma_{\pi_i}^2) \geq \theta, \\ & 0 \leq \alpha \leq 1, \end{aligned} \tag{3.45}$$

Algorithm 2 Proposed Resource Allocation Algorithm

procedure SUB-OPTIMAL TSR
  Initialize α; θ; η; P_T; $P' \leftarrow 0$; $R' \leftarrow 0$.
  while $\alpha \leq 1$ **do**
    Obtain equivalent minimization to (3.45).
    Solve this problem analogous to (3.38).
    Calculate R using α and P.
    if $R \geq R'$ **then**
      Set $\alpha' = \alpha$; $P' = P$; $R' = R$.
      $\alpha = \alpha + \delta$.
    else
      $\alpha = \alpha + \delta$.
    end if
  end while
end procedure

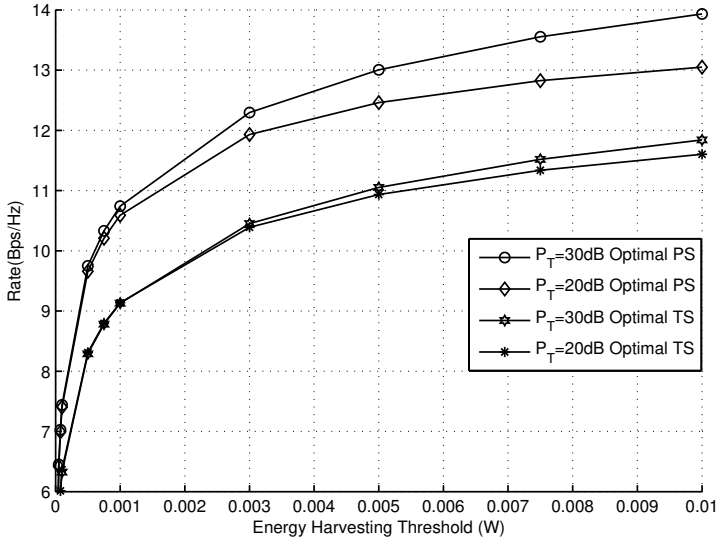

Figure 3.6 Rate versus energy harvesting threshold (θ) for different values of P_T

Following Algorithm 2, we can arrive at (α', P'), the optimal solution for (3.45).

3.5.2.3 TSR Vs PSR

The structure of (3.32) and (3.44) differs by a factor of $1-\alpha$, appearing in the objective of the latter. The range of $1-\alpha$ lies between $(0,1)$. Based on this observation, we can empirically expect the performance of PSR protocol to be superior to TSR protocol, in terms of achievable rate. In this section, we try to support this claim with the help of numerical simulations.

In Fig 3.6, we plot maximum achievable rate versus energy harvesting threshold. The corresponding results are provided for total transmit power limits of $P_T = 30$ dB and $P_T = 20$ dB, while varying the energy harvesting threshold (θ) from 1 mW to 10 mW. Next, in Fig 3.7, we plot rate versus total transmitted power of the transceivers. The total transmitted power P_T ranges from 0dB to 30dB. From these graphs, we can conclude that PSR protocol performs better than TSR protocol.

3.5.3 Relay Selection

Having solved the optimal solutions for the power allocation and PS ratio and TS ratio for PSR and TSR protocol respectively, we now address the problem of selecting the relay that results in the highest achievable rate from the set of L relays. This problem can be formulated as

$$k' = \underset{k\in\mathcal{I}}{\text{argmax}}\ R_k^*, \tag{3.46}$$

where R_k^* is the rate achieved when the kth relay is operating under optimal conditions described earlier. The optimal relay is selected as the one that leads the highest R_k^*. Combining the results, we

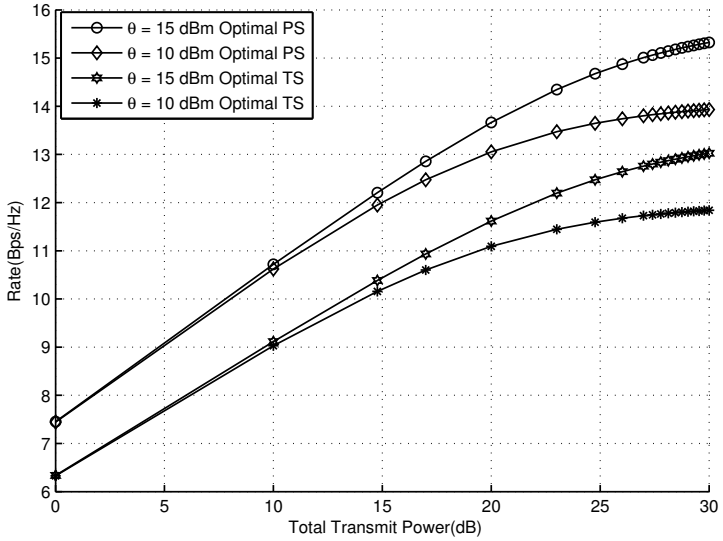

Figure 3.7 Rate versus energy harvesting threshold (θ) for different values of P_T

can represent the optimal solution to the problem in (3.31) as $(k', P_1', P_2', P_{R_{k'}}, \rho')$ and in (3.44) as $(k', P_1', P_2', P_{R_{k'}}, \alpha')$.

3.6 Summary

We considered an amplify-and-forward wireless cooperative network, where an energy constrained two-way relay node harvests energy from the received RF signal and utilizes the harvested energy to amplify-and-forward the signal to the destination node. We proposed two relaying protocols, namely, PSR protocol and TSR protocol, to enable wireless energy harvesting and information processing at the relay. We addressed the problem of optimal relay selection and resource allocation in this network. The optimal relay is selected so as to maximize the communication rate between the transceiver nodes. We proposed an optimal scheme for power allocation, relay selection, and computation of PS ratio and TS ratio in PSR and TSR protocols respectively. The performance of the proposed schemes are demonstrated via numerical simulations. From these simulations, we concluded that PSR scheme outperforms TSR scheme.

Chapter *4*

SWIET in Cooperative Cognitive Relay Networks

In this chapter, we consider the simultaneous transmission of energy and information in a cooperative CRN with two SU transceivers and a set of SU two-way relays. The SU transceivers communicate with each other through a relay, which is optimally selected from the set of L available relays. The SUs share spectrum with PU in an underlay configuration. The transmission from the SU transceivers and relays appears as interference at the PU receiver, which is kept below a threshold. The two-way relay harvests energy from the RF signals transmitted by the SU transceiver nodes and uses the harvested energy to amplify and forward the received signals. We extend the TS and PS receiver architectures to the TS relay (TSR) and PS relay (PSR) protocols to facilitate joint energy harvesting and information processing at the relay in a cognitive network. For both the TSR and PSR protocols, we address the problems of optimal power allocation, relay processing, and relay selection to maximize the sum-rate of the transceiver nodes. In both the cases, the optimization problem turns out to be a mixed-integer programming problem. We simplify this optimization problem using high SINR approximation of the instantaneous sum-rate and obtain closed-form solutions.

This chapter is organized as follows. The next section introduces the current state of the art in SWIET using relays. Section 4.2 provides an explanation of the system model. Section 4.3 describes the problem of overall rate maximization and its solution. Section 4.4 addresses the problem of maximization of the total harvested energy and its solution. Section 4.5 comprises of simulation results for the proposed algorithms. Finally, section 4.6 provides the summary of this chapter.

4.1 Introduction

Rapid advances in wireless communication technology and the huge spurt in the demand for wireless services has resulted in the limited radio spectrum growing scarce. However, most of the licensed bands remain unoccupied for a period of time [28]. This observation encouraged research in the fields of cooperative spectrum sharing mechanisms. The cognitive radio (CR) technology boosts the spectrum utilization by allowing the secondary users (SUs) to share the same band licensed to the PU, provided the interference produced at PU receiver by SU transmission is within a tolerance limit. This interfer-

ence constraints restricts the SUs to operate with low transmit power, hence the performance of SUs becomes limited. The aforementioned cooperative relaying techniques can enhance the rate and range of communication among the SUs, while keeping the interference to the PUs minimal [29].

The combination of cognitive spectrum sharing and opportunistic energy harvesting has been studied in [30], where the authors have studied the maximum secondary network throughput under given outage probability constraints. Outage performance of relay-assisted SUs, which harvest energy from the PU signal in an underlay network, is studied in [31]. In [32], a spectrum sensing technique has been proposed in order to maximize the throughput of the secondary network employing an EH relay. Relay selection and outage analysis in a cooperative CRN with EH is discussed in [33]. Resource allocation problem for EH based cooperative overlay CRN with multiple PUs and multiple SUs is studied in [34].

4.2 System Model

The SU network consists of two transceivers, T_1 and T_2, which communicate through an energy constrained intermediate AF relay node selected from a set of L relay nodes. All the devices that make up this system have a single antenna. The relays receive a compound signal, which is a blend of both energy and information, from the transceivers. To help the SU relays to handle the process of EH and transmitting the information to the destination, we look into two popular relaying protocols: PSR protocol and TSR protocol. We provide the specifics of the aforementioned relaying protocols in the next section.

4.3 PSR Protocol for CRN

The structure for this protocol is similar to the PSR protocol discussed in the previous chapter for the relaying network, and the reader can refer to Fig 3.2, to follow the discussion that unfolds in this section. The transceivers T_1 and T_2 transmit the symbols $x_1 \in \mathbb{C}$ and $x_2 \in \mathbb{C}$ in the first slot. The relays collect this signal, and the expression for the signal received by the ith relay (r_i) is

$$r_i = \sqrt{P_1} h_i x_1 + \sqrt{P_2} g_i x_2 + \gamma_i + \delta_i, \quad 1 \leq i \leq L. \tag{4.1}$$

The parameters P_1 and P_2 in the equation (4.1) represent the transmit powers of the transceivers (T_1, T_2) in the SU network, h_i, and g_i stand for the channel gains from T_1 and T_2 to the ith relay. The term γ_i ($\gamma_i \sim \mathcal{CN}(0, \sigma^2_{\gamma_i})$) represents the interference resulting from the PU transmission at the relay, and δ_i ($\delta_i \sim \mathcal{CN}(0, \sigma^2_{\delta_i})$) denotes the Gaussian noise at the relay.

As one expects from the power splitting protocol the power received at the relay is split into two parts: $\sqrt{\rho} r_i$ and $\sqrt{1-\rho} r_i$. The relay harvests energy from the first part ($\sqrt{\rho} r_i$) and the harvested power at the relay, denoted by $P_{EH}(\rho)$, can be expressed as

$$P_{EH}(\rho) = \rho\eta \mathbb{E}\{|r_i|^2\} = \rho\eta[P_1|h_i|^2 + P_2|g_i|^2 + \sigma^2_{\gamma_i} + \sigma^2_{\delta_i}]. \tag{4.2}$$

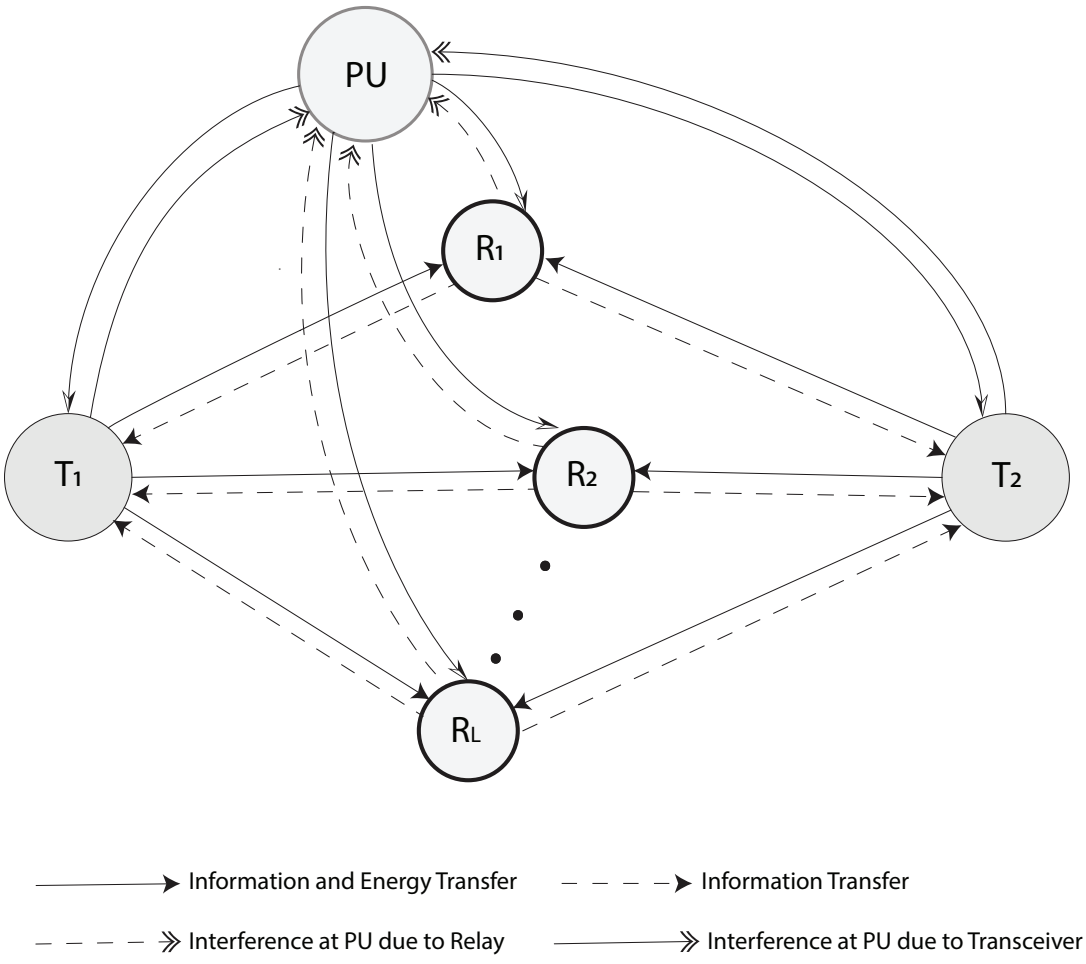

Figure 4.1 Cognitive Two-way SWIET-enabled-relaying Networks.

The remaining part of the received signal ($\sqrt{1-\rho}r_i$) is retransmitted by the relay after amplifying it by a complex number. Now, the signal received by the transceiver T_1 can be written as

$$y_1 = \sqrt{1-\rho}[\sqrt{P_1}w_i h_i h_i x_1 + \sqrt{P_2}w_i g_i h_i x_2 + w_i h_i \gamma_i + w_i h_i \delta_i] + \nu_1 + \phi_1, \tag{4.3}$$

where $w_i \in \mathbb{C}$ is the amplification factor or weight coefficient of the ith relay, $\nu_1 \sim \mathcal{CN}(0, \sigma^2_{\nu_1})$ represents the interference at T_1 due to PU transmission, and ϕ_1 represents the AWGN at transceiver T_1 with zero mean and variance $\sigma^2_{\phi_1}$. The signal received by the transceiver T_2 is given by

$$y_2 = \sqrt{1-\rho}[\sqrt{P_1}w_i h_i g_i x_1 + \sqrt{P_2}w_i g_i g_i x_2 + w_i g_i \gamma_i + w_i g_i \delta_i] + \nu_2 + \phi_2, \tag{4.4}$$

where $\nu_2 \sim \mathcal{CN}(0, \sigma^2_{\nu_2})$ represents interference at T_2 due to PU transmission, and ϕ_2 represents the AWGN at transceiver T_2 with zero mean and variance $\sigma^2_{\phi_2}$. After canceling the self-interference terms from (4.3) and (4.4), the SINR at transceiver T_1 is given by

$$SINR_{i,1} = \frac{(1-\rho)P_2|w_i|^2|h_i|^2|g_i|^2}{(1-\rho)\left[\sigma^2_{\pi_i}|w_i|^2|h_i|^2\right] + \sigma^2_{\lambda_1}}, \tag{4.5}$$

and the SINR at transceiver T_2 is given by

$$SINR_{i,2} = \frac{(1-\rho)P_1|w_i|^2|h_i|^2|g_i|^2}{(1-\rho)\left[\sigma^2_{\pi_i}|w_i|^2|g_i|^2\right] + \sigma^2_{\lambda_2}}, \tag{4.6}$$

where $\sigma^2_{\pi_i} = \sigma^2_{\gamma_i} + \sigma^2_{\delta_i}$ and $\sigma^2_{\lambda_j} = \sigma^2_{\nu_j} + \sigma^2_{\phi_j}, j = 1, 2$.
The power available at the ith relay after EH can be expressed as

$$P_{Ri} = \mathbb{E}\{|w_i\sqrt{1-\rho}r_i|^2\} \tag{4.7}$$

$$= (1-\rho)[P_1|w_i|^2|h_i|^2 + P_2|w_i|^2|g_i|^2 + |w_i|^2\sigma^2_{\pi_i}], \tag{4.8}$$

from (4.8), we have

$$|w_i| = \frac{\sqrt{P_{Ri}}}{\sqrt{(1-\rho)[P_1|h_i|^2 + P_2|g_i|^2 + \sigma^2_{\pi_i}]}}. \tag{4.9}$$

The SINR at the transceivers T_1 and T_2 in terms of P_{Ri} is given by:

$$SINR_{1,i} = \frac{P_2 P_{Ri}|h_i|^2|g_i|^2}{P_{Ri}\sigma^2_{\pi_i}|h_i|^2 + \sigma^2_{\delta_1}(P_1|h_i|^2 + P_2|g_i|^2 + \sigma^2_{\pi_i})}, \tag{4.10}$$

$$SINR_{2,i} = \frac{P_1 P_{Ri}|h_i|^2|g_i|^2}{P_{Ri}\sigma^2_{\pi_i}|g_i|^2 + \sigma^2_{\delta_2}(P_1|h_i|^2 + P_2|g_i|^2 + \sigma^2_{\pi_i})}. \tag{4.11}$$

The transmission from the SU transceiver nodes in the first slot causes interference at the PU. The interference resulting from T_1 and T_2, denoted by I_1 and I_2 respectively, are given by

$$I_1 = P_1|\hat{h}|^2, I_2 = P_2|\hat{g}|^2. \tag{4.12}$$

Here, $\hat{h}$ denotes the channel gain from T_1 to PU, similarly, $\hat{g}$ represents the gain from T2 to PU. The transmission from the relay in the second slot also causes interference at the relay given by

$$I_{R_i} = P_{R_i}|\hat{f}_i|^2. \tag{4.13}$$

Here $\hat{f}_i$ represents the channel gain from i^{th} relay to PU.

4.4 TSR Protocol for CRN

The reader can refer Fig. 3.3 to understand the structure of this protocol. In TS the receiver does EH for a fraction of the transmission time and does information processing for the remaining time. As per the commonly used convention, αT denotes the EH phase, and $(1-\alpha)$T represents the information processing phase. The information processing phase consists of two parts: Transceiver to relay transmission takes place in the first half, and in the latter half the relay transmits the signal to the destination. The signal received by the ith relay node, denoted by r_i, can be expressed as

$$r_i = \sqrt{P_1}h_i x_1 + \sqrt{P_2}g_i x_2 + \gamma_i + \delta_i, \quad 1 \leq i \leq L. \tag{4.14}$$

Energy is harvested from the received signal for a duration of αT, and the harvested power at relay node can be expressed as

$$P_{EH}(\alpha) = \alpha\eta\mathbb{E}\{|r_i|^2\} = \alpha\eta[P_1|h_i|^2 + P_2|g_i|^2 + \sigma^2_{\gamma_i} + \sigma^2_{\delta_i}]. \tag{4.15}$$

During the information receiving phase, the signal received by the relay is same as (4.14), but received in a different time duration. The signal received by the relay is re-transmitted after amplifying it by a complex number. The amplified signal received by the transceiver T_1 can be written as

$$y_1 = \sqrt{P_1}w_i h_i h_i x_1 + \sqrt{P_2}w_i g_i h_i x_2 + w_i h_i \gamma_i + w_i h_i \delta_i + \nu_1 + \phi_1, \tag{4.16}$$

The signal received by the transceiver T_2 is given by

$$y_2 = \sqrt{P_1}w_i h_i g_i x_1 + \sqrt{P_2}w_i g_i g_i x_2 + w_i g_i \gamma_i + w_i g_i \delta_i + \nu_2 + \phi_2, \tag{4.17}$$

The SINR at transceiver T_1 after self-interference cancellation is given by

$$SINR_{i,1} = \frac{P_2|w_i|^2|h_i|^2|g_i|^2}{\sigma^2_{\pi_i}|w_i|^2|h_i|^2 + \sigma^2_{\lambda_1}}, \tag{4.18}$$

and the SINR at transceiver T_2 is given by

$$SINR_{i,2} = \frac{P_1|w_i|^2|h_i|^2|g_i|^2}{\sigma^2_{\pi_i}|w_i|^2|g_i|^2 + \sigma^2_{\lambda_2}}, \tag{4.19}$$

The transmit power of the ith relay can be expressed as

$$P_{Ri} = \mathbb{E}\{|w_i r_i|^2\} = P_1|w_i|^2|h_i|^2 + P_2|w_i|^2|g_i|^2 + |w_i|^2\sigma^2_{\pi_i}, \tag{4.20}$$

from (4.20), we have

$$|w_i| = \frac{\sqrt{P_{Ri}}}{\sqrt{P_1|h_i|^2 + P_2|g_i|^2 + \sigma^2_{\pi_i}}}. \tag{4.21}$$

The SINR at the transceivers T_1 and T_2 in terms of P_{Ri} is given by:

$$SINR_{1,i} = \frac{P_2 P_{Ri}|h_i|^2|g_i|^2}{P_{Ri}\sigma^2_{\pi_i}|h_i|^2 + \sigma^2_{\delta_1}(P_1|h_i|^2 + P_2|g_i|^2 + \sigma^2_{\pi_i})}, \tag{4.22}$$

$$SINR_{2,i} = \frac{P_1 P_{Ri} |h_i|^2 |g_i|^2}{P_{Ri}\sigma_{\pi_i}^2 |g_i|^2 + \sigma_{\delta_2}^2 (P_1 |h_i|^2 + P_2 |g_i|^2 + \sigma_{\pi_i}^2)}. \tag{4.23}$$

During the energy harvesting phase, secondary transceiver nodes causes interference at the PU. The interference resulting from T_1 and T_2, denoted by I_1 and I_2 respectively, are given by

$$I_1 = P_1 |\hat{h}|^2, I_2 = P_2 |\hat{g}|^2, \tag{4.24}$$

where $\hat{h}$ and $\hat{g}$ represents the channel gain to PU from T_1 and T_2 respectively. The transceiver nodes transmit the same signal during the information transmission phase, hence the interference at the PU is same as I_1 and I_2. In the next slot, the transmission from the relay causes interference at the PU denoted by

$$I_{R_i} = P_{R_i} |\hat{f}_i|^2, \tag{4.25}$$

where $\hat{f}_i$ is the channel gain from i^{th} relay to PU.

4.5 Relay Selection and Resource Allocation

In this section we give a detailed account of overall problem formulation, and the proposed solutions. The objective of the problem is to maximize the overall rate under energy-harvesting, transmit power and PU interference constraints.

$$\max_{k \in \mathcal{I}, (P_1, P_2, P_{R_k,\xi}) \in \Lambda} \quad R_k, \tag{4.26}$$

Since only one relay will be operating at any given time, this optimization can be performed in two simple steps; first over the transmit powers and the variable ξ and then over the relay indices, as given below:

$$\max_{k \in 1,2,\ldots,L} \quad \max_{P_1, P_2, P_{R_k,\xi} \in \Lambda} \quad R_k. \tag{4.27}$$

Consequently, first we maximize the rate with respect to the variable ξ and transceiver transmit powers. We consider this rate maximization problem in both PSR and TSR protocols in the following sections.

4.5.1 Resource Allocation in PSR Protocol

The instantaneous achievable rate of the network with two-way relaying is given by

$$R_i = \frac{1}{2} \log(1 + SINR_{i,1}) + \frac{1}{2} \log(1 + SINR_{i,2}) \tag{4.28}$$

The factor $\frac{1}{2}$ used in (4.28) results from the two time slots required to complete the information exchange between the SU transceivers. In order to make the mathematical analysis more viable, we follow the

following high-SINR approximation of the rate:

$$\begin{aligned} R_i &\approx \frac{1}{2}\log\left(\frac{P_2 P_{Ri}|h_i|^2|g_i|^2}{P_{Ri}\sigma_{\pi_i}^2|h_i|^2 + \sigma_{\delta_1}^2(P_1|h_i|^2 + P_2|g_i|^2 + \sigma_{\pi_i}^2)}\right) \\ &+ \frac{1}{2}\log\left(\frac{P_1 P_{Ri}|h_i|^2|g_i|^2}{P_{Ri}\sigma_{\pi_i}^2|g_i|^2 + \sigma_{\delta_2}^2(P_1|h_i|^2 + P_2|g_i|^2 + \sigma_{\pi_i}^2)}\right) \\ &= \frac{1}{2}\log\left(\frac{P_1 P_2 P_{R_i}^2|h_i|^4|g_i|^4}{X_i Y_i}\right), \end{aligned} \tag{4.29}$$

where

$$X_i = P_{Ri}\sigma_{\pi_i}^2|h_i|^2 + \sigma_{\delta_1}^2(P_1|h_i|^2 + P_2|g_i|^2 + \sigma_{\pi_i}^2), \tag{4.30}$$

$$Y_i = P_{Ri}\sigma_{\pi_i}^2|g_i|^2 + \sigma_{\delta_2}^2(P_1|h_i|^2 + P_2|g_i|^2 + \sigma_{\pi_i}^2). \tag{4.31}$$

This high SINR approximation can significantly simplify the optimal power allocation and PS ratio computation, which can now be reformulated as

$$\begin{aligned} \max_{P_1,P_2,P_{Ri},\rho} \quad & \frac{1}{2}\log\left(\frac{P_1 P_2 P_{Ri}^2|h_i|^4|g_i|^4}{X_i Y_i}\right) \\ \text{s.t.} \quad & P_{R_i} \le P_U, P_1 \le U_1, P_2 \le U_2, \\ & I_1 + I_2 \le \epsilon, I_{R_i} \le \epsilon, \\ & P_{EH}(\rho) \ge \theta, \\ & 0 \le \rho \le 1, \end{aligned} \tag{4.32}$$

where P_U is the upper limit on the relay transmit power, U_1 and U_2 represent the transmit power budgets of T_1 and T_2 respectively, ϵ denotes the maximum interference produced due to SU transmission that PU can tolerate, and θ is the minimum amount of energy to be harvested at the relay.

The logarithm function in the problem (4.32) is an increasing function of the variable P_{Ri}. Since P_{Ri} is already a bounded variable, the optimal value of it that maximizes (4.32) can be easily deduced to be $P'_{Ri} = min(P_U, \frac{\epsilon}{|\hat{f}_i|^2})$. Here P'_{Ri} represents the optimal value of P_{Ri}. Having realized the optimal value of P_{Ri}, we proceed to compute the optimal value of (P_1, P_2, ρ) by considering only PU interference and energy harvesting constraints. Then, the problem in (4.32) can be stated as follows:

$$\begin{aligned} \max_{P_1,P_2,\rho} \quad & \frac{1}{2}\log\left(\frac{P_1 P_2 {P'_{Ri}}^2|h_i|^4|g_i|^4}{X'_i Y'_i}\right) \\ \text{s.t.} \quad & I_1 + I_2 \le \epsilon, \\ & P_{EH}(\rho) \ge \theta, \\ & 0 \le \rho \le 1, \end{aligned} \tag{4.33}$$

where X'_i and Y'_i are obtained from X_i and Y_i, respectively, by replacing P_{Ri} with P'_{Ri} in (4.30) and (4.31). Since the logarithmic function is a monotonically increasing function, the maximization in (4.33)

is equivalent to the following minimization problem:

$$\begin{aligned} \min_{P_1,P_2,\rho} \quad & \frac{X_i' Y_i'}{P_1 P_2 {P'_{Ri}}^2 |h_i|^4 |g_i|^4} \\ \text{s.t.} \quad & I_1 + I_2 \leq \epsilon, \\ & P_{EH}(\rho) \geq \theta, \\ & 0 \leq \rho \leq 1, \end{aligned} \tag{4.34}$$

We propose two closed form solutions to this problem (4.34); optimal solution and a low complexity sub-optimal solution.

4.5.1.1 Optimal Scheme

We obtain optimal power allocation and power splitting ratio using the Karush-Kuhn-Tucker conditions. In order to facilitate further analysis, we rewrite (4.34) as follows:

$$\begin{aligned} \min_{P_1,P_2,\rho} \quad & \frac{(a_1 + b_1 P_1 + c_1 P_2)(a_2 + b_2 P_1 + c_2 P_2)}{P_1 P_2} \\ \text{s.t.} \quad & uP_1 + vP_2 \leq \epsilon, \\ & \rho(mP_1 + nP_2 + q) \geq \theta, \\ & 0 \leq \rho \leq 1, \end{aligned} \tag{4.35}$$

where

$$a_1 = \frac{\sigma^2_{\pi_i}}{|g_i|^2}\left[1 + \frac{\sigma^2_{\delta_1}}{P'_{Ri}|h_i|^2}\right], \quad a_2 = \frac{\sigma^2_{\pi_i}}{|h_i|^2}\left[1 + \frac{\sigma^2_{\delta_2}}{P'_{Ri}|g_i|^2}\right], b_1 = \frac{\sigma^2_{\delta_1}}{P'_{Ri}|g_i|^2}, \quad b_2 = \frac{\sigma^2_{\delta_2}}{P'_{Ri}|g_i|^2}, \quad c_1 = \frac{\sigma^2_{\delta_1}}{P'_{Ri}|h_i|^2},$$
$$c_2 = \frac{\sigma^2_{\delta_2}}{P'_{Ri}|h_i|^2}, \quad m = \eta|h_i|^2, \quad n = \eta|g_i|^2, q = \eta\sigma^2_{\pi_i}, u = |\hat{h}|^2, \quad \text{and} \quad v = |\hat{g}|^2.$$

Then, the Lagrangian associated with the problem in (4.35) is given by

$$\mathcal{L}(P_1, P_2, \rho, \mu) = f + \mu_1[\theta - \rho(mP_1 + nP_2 + q)] + \mu_2(uP_1 + vP_2 - \epsilon) + \mu_3(\rho - 1) - \mu_4\rho,$$

where $f = \frac{(a_1+b_1P_1+c_1P_2)(a_2+b_2P_1+c_2P_2)}{P_1P_2}$ and $\{\mu_i\}_{i=1}^4$ are the Lagrangian multipliers. The optimal solution satisfies the following KKT conditions:

$$\frac{\partial f}{\partial P_1} - \mu_1\rho m + \mu_2 u = 0, \ \frac{\partial f}{\partial P_2} - \mu_1\rho n + \mu_2 v = 0, \mu_1[\theta - \rho(mP_1 + nP_2 + q)] = 0, \mu_2(uP_1 + vP_2 - \epsilon) = 0,$$
$$\mu_3(\rho - 1) = 0, \ \mu_4\rho = 0, \ \mu_i \geq 0, \ i = 1, 2, 3, 4.$$

By solving the set of KKT conditions given above, we obtain the optimal values of P_1, P_2, and ρ as follows:

$$P_1' = \frac{\epsilon\left[r_3\sqrt{1+\frac{r_1+r_2}{r_3}+\frac{r_1 r_2}{r_3^2}}-(r_2+r_3)\right]}{u(r_1-r_2)}, \tag{4.36}$$

$$P_2' = \frac{\epsilon\left[(r_1+r_3)-r_3\sqrt{1+\frac{r_1+r_2}{r_3}+\frac{r_1 r_2}{r_3^2}}\right]}{v(r_1-r_2)}, \tag{4.37}$$

$$\rho' = \frac{\theta}{\eta(P_1^{\backprime}|h_i^2| + P_2^{\backprime}|g_i|^2 + \sigma_{\pi_i}^2)}, \tag{4.38}$$

where $r_1 = \frac{vb_1b_2}{u} + \frac{va_1b_2}{\epsilon} + \frac{va_2b_1}{\epsilon}$, $r_2 = \frac{uc_1c_2}{v} + \frac{ua_1c_2}{\epsilon} + \frac{ua_2c_1}{\epsilon}$, and $r_3 = \frac{uva_1a_2}{\epsilon^2}$.

Having solved the subproblem, we proceed to solve the optimal power allocation problem (4.32). To get this solution, we should place the transmit power limits on the results of the problem (4.33). Then the overall solution for (4.32) can be stated as follows:

$$(P_{R_i}^*, P_1^*, P_2^*, \rho^*) = \begin{cases} (P^{'}, P_1', P_2', \rho'), \\ \quad \text{if } P_1' \le U_1, P_1' \le U_2 \\ (P^{'}, min(P_T - U_2, U_1), U_2, \rho'), \\ \quad \text{if } P_1' < U_1, P_1' > U_2 \\ (P^{'}, U_1, min(P_T - U_1, U_2), \rho'), \\ \quad \text{if } P_1' > U_1, P_1' < U_2 \\ (P^{'}, U_1, U_2, \rho'), \\ \quad \text{if } P_1' > U_1, P_1' > U_2 \end{cases}$$

where $P^{'} = min(P_U, \frac{\epsilon}{|\hat{f}_i|^2})$.

4.5.1.2 Sub-optimal Scheme

Here,we propose a simplified sub-optimal scheme for computing power allocation and power-splitting ratio. In this sub-optimal scheme, we consider a trivial power allocation such that $P_1 = P_2 = P$. Let U denote the upper bound on P, now the problem in (4.32) is equivalent to follows:

$$\begin{aligned} \max_{P,\rho} \quad & \frac{1}{2}\log\left(\frac{P^2 {P_{Ri}^{'}}^2 |h_i|^4 |g_i|^4}{\hat{X}_i' \hat{Y}_i'}\right) \\ \text{s.t.} \quad & P \le U, \\ & P(|\hat{h}|^2 + |\hat{g}|^2) \le \epsilon, \\ & \eta\rho(P(|h_i|^2 + |g_i|^2) + \sigma_{\pi_i}^2) \ge \theta, \\ & 0 \le \rho \le 1, \end{aligned} \tag{4.39}$$

where

$$\hat{X_i}' = P'_{Ri}\sigma^2_{\pi_i}|h_i|^2 + \sigma^2_{\delta_1}(P(|h_i|^2 + |g_i|^2) + \sigma^2_{\pi_i}), \tag{4.40}$$

$$\hat{Y_i}' = P'_{Ri}\sigma^2_{\pi_i}|g_i|^2 + \sigma^2_{\delta_2}(P(|h_i|^2 + |g_i|^2) + \sigma^2_{\pi_i}). \tag{4.41}$$

We can use the monotonically increasing nature of the logarithmic function to convert (4.39) into the minimization problem (4.42), to simplify the complexity.

$$\begin{aligned} \min_{P,\rho} \quad & \left(\frac{e_1}{P} + f_1\right)\left(\frac{e_2}{P} + f_2\right) \\ \text{s.t.} \quad & P \leq U, \\ & P(|\hat{h}|^2 + |\hat{g}|^2) \leq \epsilon, \\ & \eta\rho(P(|h_i|^2 + |g_i|^2) + \sigma^2_{\pi_i}) \geq \theta, \\ & 0 \leq \rho \leq 1, \end{aligned} \tag{4.42}$$

Here $e_1 = \frac{P'_{Ri}\sigma^2_{\pi_i}|h_i|^2 + \sigma^2_{\pi_i}\sigma^2_{\delta_1}}{P'_{R_i}|h_i|^2|g_i|^2}$, $e_2 = \frac{P'_{Ri}\sigma^2_{\pi_i}|g_i|^2 + \sigma^2_{\pi_i}\sigma^2_{\delta_2}}{P'_{R_i}|h_i|^2|g_i|^2}$, $f_1 = \frac{\sigma^2_{\delta_1}(|h_i|^2 + |g_i|^2)}{P'_{R_i}|h_i|^2|g_i|^2}$, and $f_2 = \frac{\sigma^2_{\delta_2}(|h_i|^2 + |g_i|^2)}{P'_{R_i}|h_i|^2|g_i|^2}$. We can observe that the objective function in the problem given above is minimized when P takes the maximum value. From the constraints we can infer the optimal value of P to be $P^* = min(\frac{\epsilon}{|\hat{h}|^2+|\hat{g}|^2}, U)$. when $\rho' = \frac{\theta}{\eta(P^*(|h_i^2|+|g_i|^2)+\sigma^2_{\pi_i})}$, then the minimum value of the objective function in (4.42) is given by $\left(\frac{e_1}{P^*} + f_1\right)\left(\frac{e_2}{P^*} + f_2\right)$.

4.5.2 Resource Allocation in TSR Protocol

The instantaneous achievable rate of the wireless co-operative network with two-way relaying is given by

$$R_i = \frac{1-\alpha}{2}\log(1 + SINR_{i,1}) + \frac{1-\alpha}{2}\log(1 + SINR_{i,2}). \tag{4.43}$$

The factor of $\frac{1-\alpha}{2}$ used in (4.43), results from the two time slots required to complete the information exchange between the SU transceivers. We follow the high-SINR approximation of the rate:

$$\begin{aligned} R_i &\approx \frac{1-\alpha}{2} \times \left\{ \log\left(\frac{P_2 P_{Ri}|h_i|^2|g_i|^2}{P_{Ri}\sigma^2_{\pi_i}|h_i|^2 + \sigma^2_{\delta_1}(P_1|h_i|^2 + P_2|g_i|^2 + \sigma^2_{\pi_i})}\right) \right. \\ &\quad \left. + \log\left(\frac{P_1 P_{Ri}|h_i|^2|g_i|^2}{P_{Ri}\sigma^2_{\pi_i}|g_i|^2 + \sigma^2_{\delta_2}(P_1|h_i|^2 + P_2|g_i|^2 + \sigma^2_{\pi_i})}\right)\right\} \\ &= \frac{1-\alpha}{2}\log\left(\frac{P_1 P_2 P^2_{R_i}|h_i|^4|g_i|^4}{X_i Y_i}\right), \end{aligned} \tag{4.44}$$

where

$$X_i = P_{Ri}\sigma^2_{\pi_i}|h_i|^2 + \sigma^2_{\delta_1}(P_1|h_i|^2 + P_2|g_i|^2 + \sigma^2_{\pi_i}), \tag{4.45}$$

$$Y_i = P_{Ri}\sigma^2_{\pi_i}|g_i|^2 + \sigma^2_{\delta_2}(P_1|h_i|^2 + P_2|g_i|^2 + \sigma^2_{\pi_i}). \tag{4.46}$$

As in the case of PSR protocol, we can use high SINR approximation to simplify the optimal power allocation and TS ratio computation, which can now be reformulated as

$$\begin{aligned} \max_{P_1,P_2,P_{Ri},\alpha} \quad & \frac{1-\alpha}{2}\log\left(\frac{P_1P_2P_{Ri}^2|h_i|^4|g_i|^4}{X_iY_i}\right) \\ \text{s.t.} \quad & P_{R_i} \leq P_U, P_1 \leq U_1, P_2 \leq U_2, \\ & I_1 + I_2 \leq \epsilon, I_{R_i} \leq \epsilon, \\ & P_{EH}(\alpha) \geq \theta, \\ & 0 \leq \alpha \leq 1. \end{aligned} \tag{4.47}$$

Let P'_{Ri} denote the optimal value of P_{Ri} then its optimal value is given by $P'_{Ri} = min(P_U, \frac{\epsilon}{|\hat{f}_i|^2})$. The same line of reasoning presented for (4.32) can be used to arrive at this result. Having realized the optimal value of P_{Ri}, we proceed to compute the optimal value of (P_1, P_2, α) by considering only PU interference and energy harvesting constraints. Then, the problem in (4.47) can be stated as follows:

$$\begin{aligned} \max_{P_1,P_2,\alpha} \quad & \frac{1-\alpha}{2}\log\left(\frac{P_1P_2{P'_{Ri}}^2|h_i|^4|g_i|^4}{X'_iY'_i}\right) \\ \text{s.t.} \quad & I_1 + I_2 \leq \epsilon, \\ & P_{EH}(\alpha) \geq \theta, \\ & 0 \leq \alpha \leq 1, \end{aligned} \tag{4.48}$$

4.5.2.1 Optimal Scheme

If α in (4.48) is a constant, we can solve this problem on the same lines as (4.33). We perform a linear search over the range of α and select the value which maximizes both the objective and satisfies the energy harvesting threshold constraint. With $\alpha = 0$ the energy harvesting threshold of (4.48) cannot be satisfied for a nonzero value of θ. So, we initialize the linear search with a value of α close to zero. Let us denote the objective of (3.44) by R and R' represents the maximum value of this objective. P'_1, P'_2 and α' represents the optimal values corresponding to R'. The proposed solution is outlined in the Algorithm3.

Following the Algorithm3, one can arrive at (P'_1, P'_2, α') the optimal solution to the problem (4.48). Now the transmit power limits can be brought back on the results of (4.48) to obtain the solution of

Algorithm 3 Proposed Resource Allocation Algorithm

procedure OPTIMAL TSR
  Initialize α; ϵ; θ; δ; $P_1' \leftarrow 0$; $P_2' \leftarrow 0$; $R' \leftarrow 0$.
  while $\alpha \leq 1$ **do**
    Solve (4.48) analogous to (4.33), obtain P_1 and P_2.
    Calculate R using P_1 and P_2.
    if $R \geq R'$ **then**
      set $\alpha' = \alpha$; $P_1' = P_1$; $P_2' = P_2$;$R' = R$.
      $\alpha = \alpha + \delta$.
    else
      $\alpha = \alpha + \delta$.
    end if
  end while
  return
end procedure

Algorithm 4 Proposed Resource Allocation Algorithm

procedure OPTIMAL TSR
  Initialize α; ϵ; θ; δ; $P_1' \leftarrow 0$; $P_2' \leftarrow 0$; $R' \leftarrow 0$.
  while $\alpha \leq 1$ **do**
    Solve the problem analogous to PSR protocol, obtain P_1 and P_2.
    Calculate R using P_1 and P_2.
    if $R \geq R'$ **then**
      set $\alpha' = \alpha$; $P_1' = P_1$; $P_2' = P_2$;$R' = R$.
      $\alpha = \alpha + \delta$.
    else
      $\alpha = \alpha + \delta$.
    end if
  end while
  return
end procedure

(4.47). The overall solution looks as follows:

$$(P^*_{R_i}, P^*_1, P^*_2, \alpha^*) = \begin{cases} (P^{'}, P^{'}_1, P^{'}_2, \alpha'), \\ \quad \text{if } P^{'}_1 \leq U_1, P^{'}_1 \leq U_2 \\ (P^{'}, min(P_T - U_2, U_1), U_2, \alpha'), \\ \quad \text{if } P^{'}_1 < U_1, P^{'}_1 > U_2 \\ (P^{'}, U_1, min(P_T - U_1, U_2), \alpha'), \\ \quad \text{if } P^{'}_1 > U_1, P^{'}_1 < U_2 \\ (P^{'}, U_1, U_2, \alpha'), \\ \quad \text{if } P^{'}_1 > U_1, P^{'}_1 > U_2 \end{cases}$$

where $P^{'} = min(P_U, \frac{\epsilon}{|\hat{f}_i|^2})$.

4.5.2.2 Sub-optimal Scheme

We simply the problem (4.47), by relaxing the power constraint to $P_1 = P_2 = P$ and now the problem (4.47) transforms into

$$\begin{aligned} \max_{P,\alpha} \quad & \frac{1-\alpha}{2} \log \left(\frac{P^2 {P^{'}_{Ri}}^2 |h_i|^4 |g_i|^4}{\hat{X}^{'}_i \hat{Y}^{'}_i} \right) \\ \text{s.t.} \quad & P \leq U, \\ & P(|\hat{h}|^2 + |\hat{g}|^2) \leq \epsilon, \\ & \eta\alpha(P(|h_i|^2 + |g_i|^2) + \sigma^2_{\pi_i}) \geq \theta, \\ & 0 \leq \alpha \leq 1, \end{aligned} \tag{4.49}$$

For a fixed value of α, we can convert (4.49) into an equivalent minimization problem:

$$\begin{aligned} \min_{P} \quad & \left(\frac{e_1}{P} + f_1\right)\left(\frac{e_2}{P} + f_2\right) \\ \text{s.t.} \quad & P \leq U, \\ & P(|\hat{h}|^2 + |\hat{g}|^2) \leq \epsilon, \\ & \eta\alpha(P(|h_i|^2 + |g_i|^2) + \sigma^2_{\pi_i}) \geq \theta, \\ & 0 \leq \rho \leq 1, \end{aligned} \tag{4.50}$$

The objective function is minimized when P is maximum. From the constraints we can infer the optimal value of P to be $\hat{P} = min(\frac{\epsilon}{|\hat{h}|^2 + |\hat{g}|^2}, U)$.

Following Algorithm 4, we can arrive at (α', P'), the optimal solution for (4.49).

Algorithm 5 Proposed Resource Allocation Algorithm

procedure SUB-OPTIMAL TSR
  Initialize α; ϵ; θ; δ; U; $P \leftarrow 0$; $R' \leftarrow 0$.
  while $\alpha \leq 1$ **do**
    For a fixed α optimal P is $\hat{P} = min(\frac{\epsilon}{|\hat{h}|^2+|\hat{g}|^2}, U)$.
    Calculate R using α and P.
    if $R \geq R'$ **then**
      Set $\alpha' = \alpha$; $P' = P$; $R' = R$.
      $\alpha = \alpha + \delta$.
    else
      $\alpha = \alpha + \delta$.
    end if
  end while
  return
end procedure

4.5.3 Optimal Relay Selection

The solution to the first part of (4.26), i.e., the resource allocation problem is worked out for both the relaying protocols. Let R_k^* denote the rate achieved when the kth relay operates with the optimal parameters obtained as the solution to the resource allocation problem. Now the second part of (4.26), i.e., the relay selection boils down to selecting the relay that delivers the maximum R_k^*. This whole affair of relay selection can be put together mathematically as follows:

$$k^* = \underset{k \in \mathcal{I}}{\text{argmax}}\ R_k^*. \tag{4.51}$$

Here, k^* denotes the index of the relay that satisfies the problem (4.51). Now, the overall solution for the problem (4.26) can be clubbed together as $(k^*, P_1^*, P_2^*, P_{R_{k^*}}^*, \rho^*)$ for the PSR protocol and as $(k^*, P_1^*, P_2^*, P_{R_{k^*}}^*, \alpha^*)$ for the TSR protocol.

4.6 Simulation Results

In this section, we illustrate the performance of the proposed joint relay selection and optimal power allocation scheme with energy harvesting through simulations. We use these simulations to draw comparisons between the performance of both PSR and TSR protocols. In all the simulations, we have assumed $\sigma_{\delta_1}^2 = \sigma_{\delta_2}^2$, $\eta = 0.7$. The value of $\sigma_{\pi_i}^2$ is assumed to be same for all the relays. We assume all channels to follow Rayleigh fading and their elements to be independent and identically distributed complex Gaussian random variables with zero mean and unit variance.

In Fig. 4.2 and Fig. 4.4 we plot rate versus ϵ for different values of P_U. The rate increases as θ increases because a larger ϵ leads to more transmit power which in turn results in a larger rate. Rate versus P_T with varying ϵ is studied in Fig. 4.3 and Fig. 4.5. Rate increases for lower values of P_T but

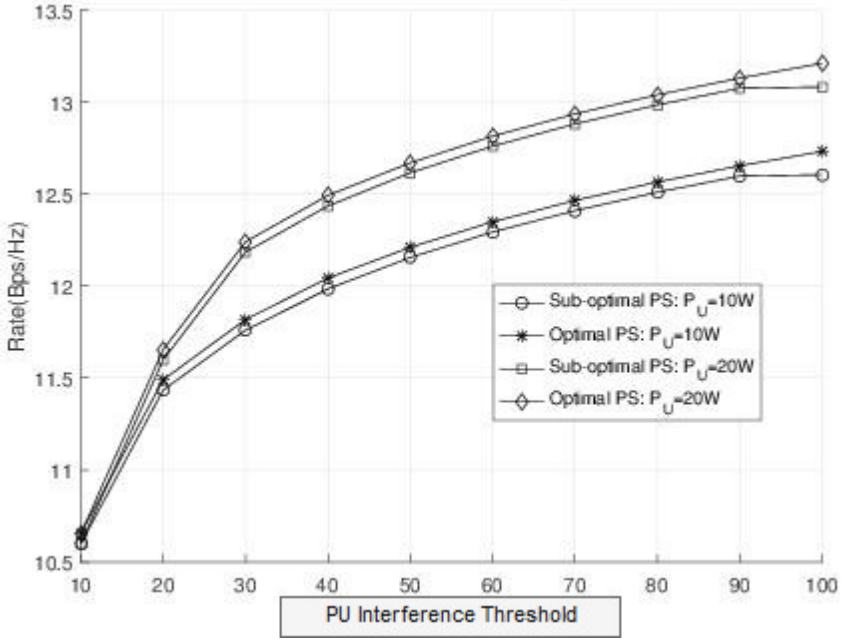

Figure 4.2 Rate vs ϵ for PSR; P_T=20dB; θ = 1mW.

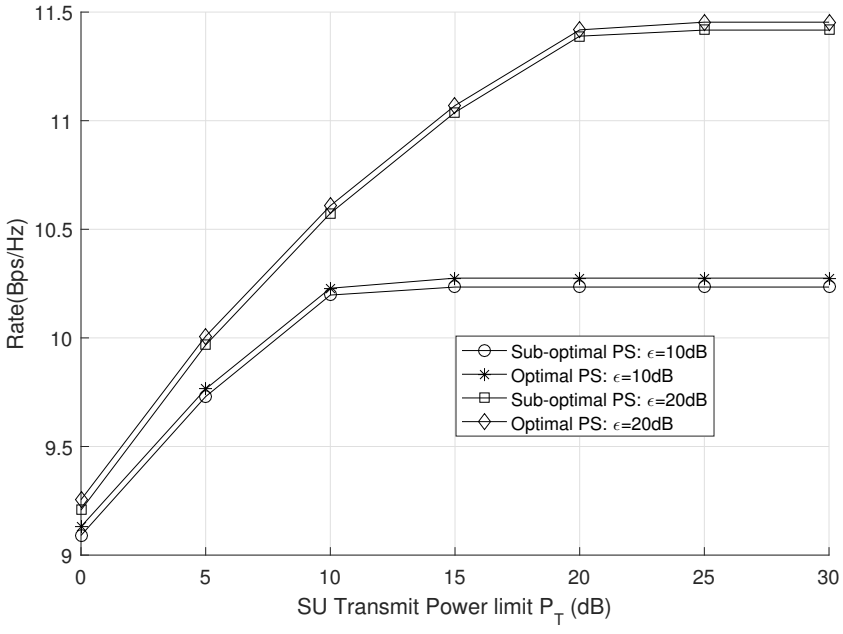

Figure 4.3 Rate vs P_T for PSR; θ=1mW; P_U = 30dB.

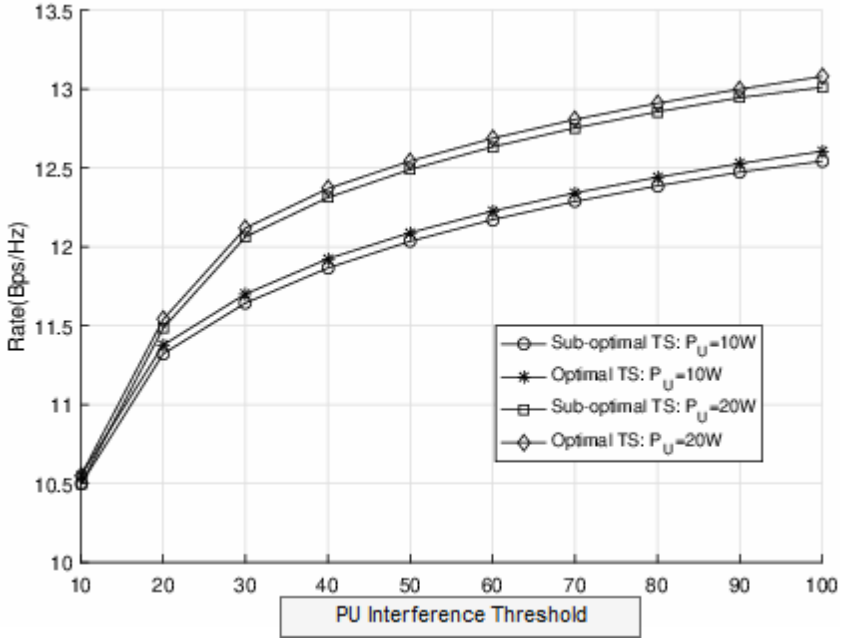

Figure 4.4 Rate vs ϵ for TSR; P_T=20dB; θ = 1mW.

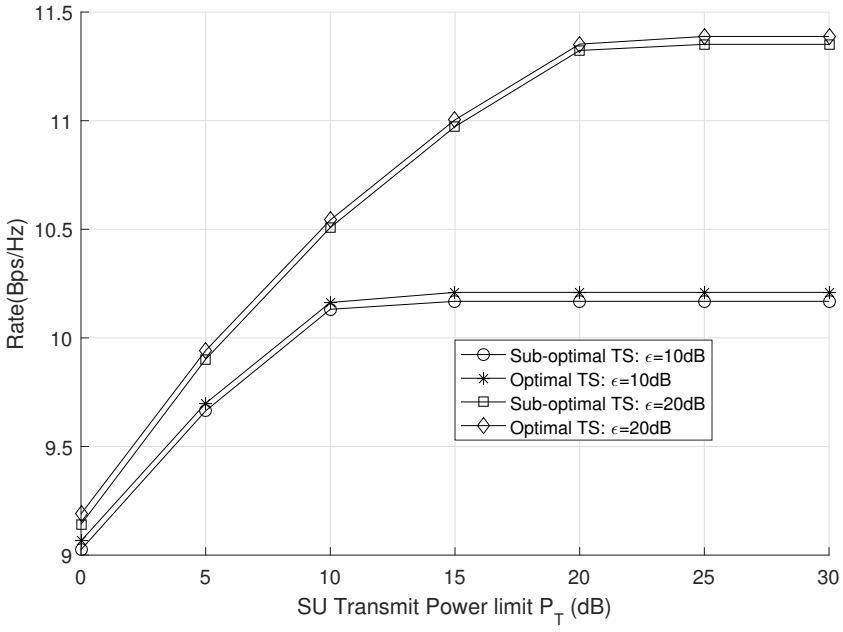

Figure 4.5 Rate vs P_T for TSR; θ=1mW; P_U = 30dB.

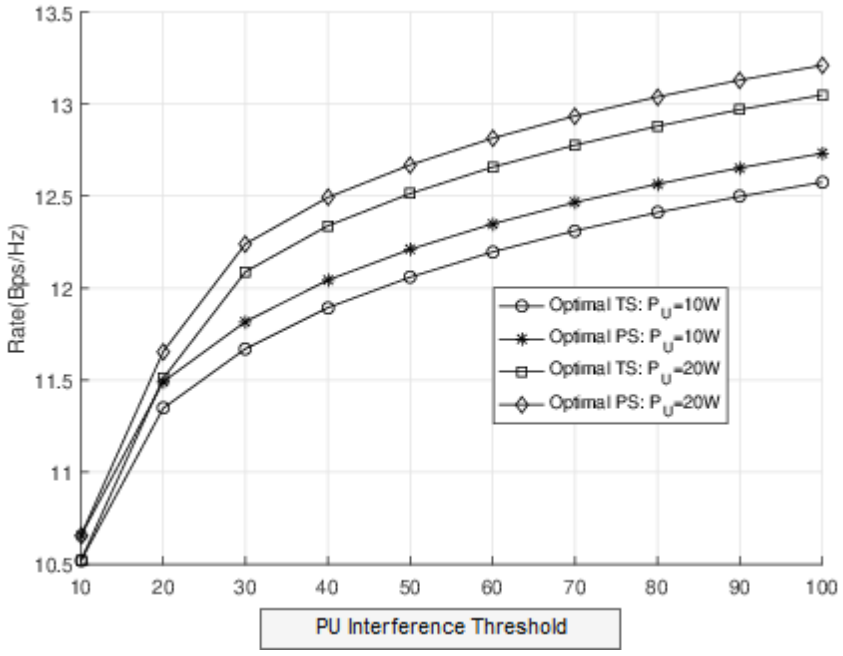

Figure 4.6 Rate vs ϵ; P_T=20dB; θ = 1mW.

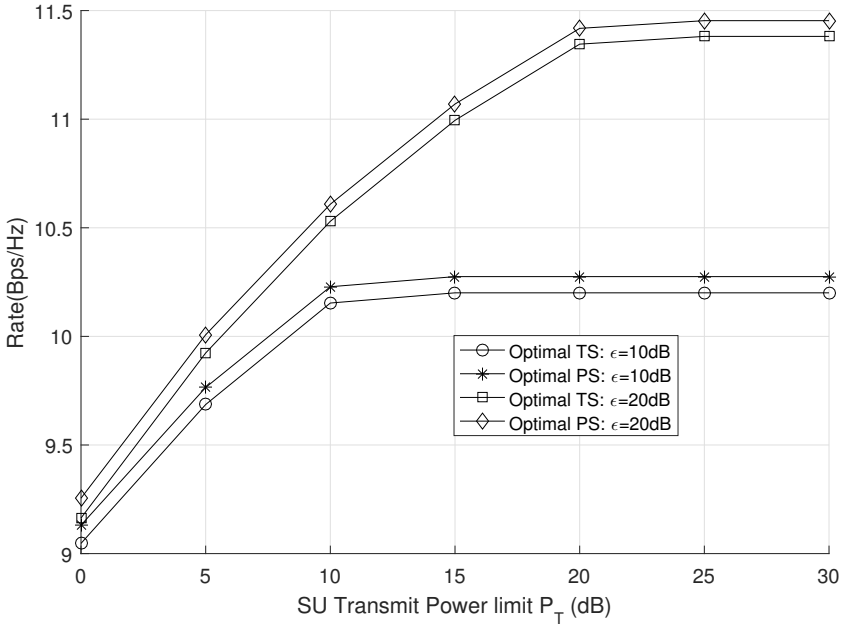

Figure 4.7 Rate vs P_T; θ=1mW; P_U = 30dB.

saturates for higher values because of the upper bound on the transmit powers. From these plots, we can also conclude that the reduced computational complexity of the proposed suboptimal scheme does not lead to significant performance degradation compared to the optimal scheme.

Next, we compare the performance of the PSR protocol with TSR protocol. In Fig. 4.6 rate versus ϵ for different values of P_U is portrayed. Similarly in Fig. 4.7 rate versus P_T with varying ϵ is plotted. The objective in the optimization problem for PSR protocol and TSR protocol differ by a factor of $1-\alpha$ which lies in the range $(0, 1)$. Based on this observation, we expect PSR protocol to outperform TSR protocol. The plots shown in Fig. 4.6 and Fig. 4.7 strongly support this.

4.7 Summary

We considered simultaneous energy and information transfer in a cooperative CRN employing a two-way relay node that operates using the energy harvested from the SU transceiver nodes. We considered two relaying protocols, namely, PSR protocol and TSR protocol, to enable wireless energy harvesting and information processing at the relay. We addressed the problem of optimal relay selection and transceiver and relay processing. The relay is selected so as to maximize the communication rate between the SU transceiver nodes. We proposed optimal and sub-optimal schemes for power allocation, relay selection, and computation of PS ratio and TS ratio in PSR and TSR protocols, respectively. Analytical solutions are obtained for the PSR scheme. The performance of the proposed schemes is demonstrated via numerical simulations. From these simulations, we concluded that PSR scheme outperforms TSR scheme. It is also observed that the proposed low-complexity suboptimal scheme performs close to the optimal scheme.

Chapter *5*

Wireless-Powered Communication Networks

The previous chapters explore SWIET in cooperative networking scenarios. In those networks, some of the nodes were jointly transferring energy and information to some other nodes. In this chapter, we study a network of battery-less devices that operate using energy received received from a central node. A network of low-power IoT's or sensors is a typical example of such a scenario. We address the problem of optimal time allocation for such a network operating in time-division duplexing mode. Furthermore, we briefly introduce the non-linear effects in energy harvesting devices and their effect on the performance of proposed algorithms.

5.1 Wireless Powered Communication

The components of this network include a hybrid access point (HAP) and k users, as shown in the figure 5.2. The HAP comes furnished with two antennas: one antenna is for transferring energy to the users in the downlink, and the other antenna receives the processed information from the users in the uplink. In this work, the channel gains for uplink and downlink channels are assumed to be different. The term f_i denotes the channel gain from the HAP to the ith user, and e_i denotes the channel gain from the ith user to the HAP. In this work, we assume that the channels remain constant in a transmission cycle and all the users have a single antenna.

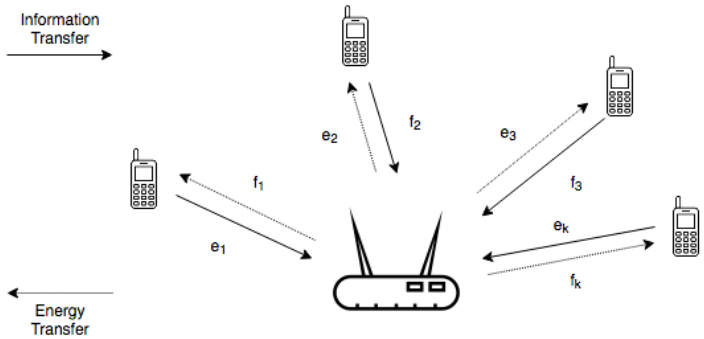

Figure 5.1 Wireless powered communication system

The HAP transmits constant power (P_H) in the downlink mode and receives information from the users in the uplink. The transmission from the users is scheduled in a time division multi-access (TDMA) manner as shown in the figure 5.2. In the figure 5.2, the term t_i denotes the transmission period of the i^{th} user. Since, the users transmit information in their dedicated slot there will be no inter user interference.

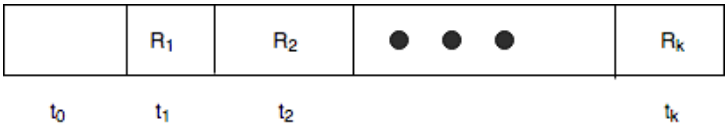

Figure 5.2 TDMA Structure

The users harvest energy continuously except in the slot in which they are transmitting information to the HAP. The total achievable throughput (Γ) for all the users in the nth transmission cycle is given by

$$\Gamma = \sum_{i=1}^{k} t_i^n R_i^n. \tag{5.1}$$

Here, R_i^n denotes the instantaneous uplink rate of user i. To calculate this instantaneous rate, we must know the signal to interference at the user. The users harvest energy from the downlink signal from the HAP till their transmission slot. Therefore, the total energy available with user i in the nth transmission cycle can be expressed as

$$E_i^n = \eta_i P_H (f_i^n \sum_{j=0}^{i-1} t_j^n + f_i^{n-1} \sum_{j=i+1}^{k} t_j^{n-1}), \tag{5.2}$$

Using (5.2), we can calculate the transmit power of the ith user, and it is given by

$$P_i^n = \frac{E_i^n}{t_i^n}, \tag{5.3}$$

Now, the instantaneous uplink rate of user i in the nth transmission cycle is given by

$$R_i^n = \log(1 + \frac{e_i^n E_i^n}{t_i^n \sigma_i^2}), \tag{5.4}$$

Here σ_i^2 represents the Gaussian noise at the user i. This value of R_i^n in (5.4) can be plugged into (5.1) to derive the complete expression for the total achievable throughput by all the users

$$\Gamma = \sum_{i=1}^{k} t_i^n \log \left(1 + \frac{e_i^n (\eta_i P_H (f_i^n \sum_{j=0}^{i-1} t_j^n + f_i^{n-1} \sum_{j=i+1}^{k} t_j^{n-1}))}{t_i^n \sigma^2} \right). \tag{5.5}$$

To measure the performance of this network we propose the sum throughput maximization problem. In order to reduce the complexity of this problem, we normalize the communication block to unity, i.e.,

$T = 1$. Here, T denotes the total time period of the communication block.

$$\begin{aligned} \max_{\tilde{\mathbf{t}}^n} \quad & \sum_{i=1}^{k} t_i^n R_i^n \\ \text{s.t.} \quad & t_i^n \geq 0, \forall i \in 0, 1, 2, ...k, \\ & \sum_{i=0}^{k} t_i^n \leq 1. \end{aligned} \tag{5.6}$$

In this problem, the term $\tilde{\mathbf{t}}^n$ is a vector of all the time intervals, i.e., $\tilde{\mathbf{t}}^n = [t_0^n, t_1^n, ...t_k^n]$.

5.1.1 Energy Causality

From equation (5.5), one can infer that the sum throughput depends on the values from the previous slot. This coupling could complicate the process of solving the optimization problem. To avoid this complication, the people who explored WPT introduced approximations to eliminate the coupling with the previous slot. For example, in [35], to avoid coupling the users are not allowed to harvest energy after their transmission slot. Therefore, the throughput remains unchanged in all the transmission cycles. The authors of [35] christened this procedure as energy causality. To differentiate the problem with energy causality from the general problem we drop the superscripts which denote the transmission cycle. The sum throughput maximization problem for the energy causality scenario is given by

$$\begin{aligned} \max_{\tilde{\mathbf{t}}} \quad & \sum_{i=1}^{k} t_i \log \left(1 + \frac{e_i \eta_i P_H f_i \sum_{j=0}^{i-1} t_j}{t_i \sigma^2} \right) \\ \text{s.t.} \quad & t_i \geq 0, \forall i \in 0, 1, 2, ...k, \\ & \sum_{i=0}^{k} t_i \leq 1. \end{aligned} \tag{5.7}$$

The Hessian matrix for the problem (5.7) is negative semidefinite, from this we can claim that this problem is a convex optimization problem [35]. For the first transmission cycle, the reader can observe that the problem (5.6) is similar to (5.7). So, we want to compare the performance of the problem (5.6) in its second transmission cycle with the problem (5.7).

5.1.2 Simulation Results

For the following simulation results, we assume that the channels undergo Rayleigh fading. From these plots, we can conclude that the performance of the general problem is better than the one with energy causality. In our future work, we want to explore the nature of the general problem and carefully analyze the metamorphosis of the coupling in various iterations of the transmission cycle.

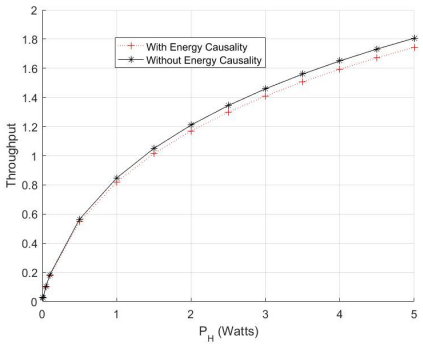

Figure 5.3 Throughput vs HAP transmit power

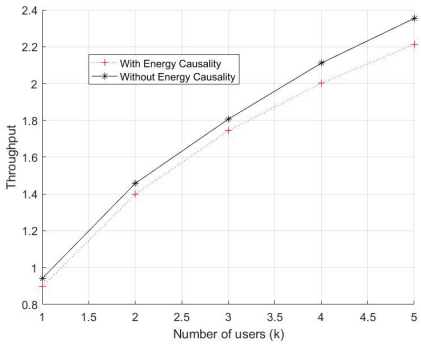

Figure 5.4 Throughput vs Users

5.2 Non Linear Energy Harvesting

The readers who have progressed through the previous chapters are familiar with the concept of energy harvesting. A keen eye might have discerned that the mathematical model used for EH in chapter 2 and 3 is linear. However, recent works in this field have suggested that the linear model cannot capture all the non-linearities present in the circuits used for RF to DC conversion [36, 37]. In this chapter, we discuss a commonly used nonlinear energy harvesting model.

$$P_{EH}^{NL} = \frac{[\psi - M\Omega]}{1 - \Omega} \tag{5.8}$$

Here

$$\Omega = \frac{1}{1 + exp(ab)}, \tag{5.9}$$

$$\psi = \frac{M}{1 + exp(-a(P_{EH} - b))}. \tag{5.10}$$

The terms a and b accounts for the hardware phenomena like leakage currents, calibration errors e.t.c. M represents the maximum power an energy harvesting circuit can harvest before it saturates. P_{EH} represents the amount of power harvested using the linear model. Experiments show that this model closely trails the practical results.

To show the disparity between the performance of linear and nonlinear energy harvesting we consider the same system model introduced at the beginning of this chapter. However, to avoid further complications, the problem with energy causality is used instead of the general problem. After integrating nonlinear energy harvesting into the problem (5.7), it turns out as follows:

$$\max_{\tilde{\mathbf{t}}} \quad \sum_{i=1}^{k} t_i \log \left(1 + \frac{\frac{M}{1+exp(-a(e_i \eta_i P_H f_i \sum_{j=0}^{i-1} t_j - b))} - M\Omega}{\frac{1-\Omega}{t_i \sigma^2}} \right) \tag{5.11}$$

$$\text{s.t.} \quad t_i \geq 0, \forall i \in 0, 1, 2, ...k,$$

$$\sum_{i=0}^{k} t_i \leq 1.$$

5.2.1 Simulation Results

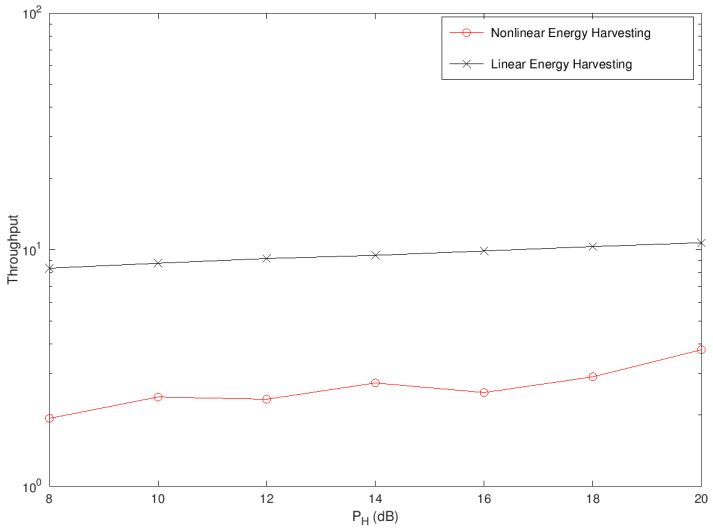

Figure 5.5 Power-Splitting Receiver Architecture

In this simulation, we use the following values for the nonlinear parameters $a = 150$, $b = 0.014$ and $M = 0.024$. The authors of the work [36] arrived at these values after carefully studying the behavior of devices. In future, we plan to integrate this nonlinear energy harvesting model into the works explored in the previous chapters to arrive values that are close to the ones obtained in practice. Observing the contrast in the performance between the linear and the nonlinear energy model from the figure we strongly feel exploring this field is necessary in order to ease the transition of research work to industry.

5.3 Summary

In this chapter, we studied wireless-powered communication networks, wherein a set of battery-less devices operate using energy received received from a central node. A network of low-power IoT's or sensors is a typical example of such a scenario. Specifically, we addressed the problem of optimal

time allocation for such a network operating in time-division duplexing mode. Furthermore, we also introduced the non-linear effects in energy harvesting devices and their effect on the performance of proposed algorithms. Simulation results were provided to demonstrate the performance of the proposed algorithms.

Chapter *6*

Conclusions

The number of devices in a network are increasing exponentially in response to the growing demand for wireless services. One promising solution to meet the energy requirements of this bulk network is energy harvesting. It allows the wireless nodes to capture ambient energy and store in a device for future use. Chapter 2 presents the techniques used to realize WET in practice. The main focus, however, is on EH using the RF signals as they are instrumental in achieving SWIET. In the same chapter, the reader can find details about the practical receiver structures to handle SWIET and the mechanism the wireless nodes use to convert RF signals to DC.

Chapter 3 of this work explores SWIET in a wireless cooperative relaying network. In this network, the relays use amplify-and-forward (AF) scheme to amplify and retransmit the signals to their respective destination. These relays extract the energy required for amplification from the received radio frequency (RF) signals. To facilitate this process, we proposed two relaying protocols, namely, TSR protocol and PSR protocol. For these protocols, we addressed the problem of optimal resource allocation and relay selection. In the context of rate maximization, the performance of PSR protocol in a WCRN is better than TSR protocol.

For all the positive attributes in a WCRN like connectivity, diversity e.t.c it is not adept in providing a mechanism to improve the spectral efficiency of the network. So, we turn our attention to CRN, which employ spectrum sharing to boost the overall spectral efficiency of the system. Chapter 4 of this work examines a CRN with an added SWIET functionality. The SUs of this network share the spectrum with a PU in an underlay fashion and their communication is supported by a set of AF relays. The performance of this network with respect to rate maximization for different relaying protocols is studied. Observing the closed form solutions and the numerical simulations obtained for the rate maximization problem, we conclude that the PSR protocol outshines TSR protocol.

In chapter 5, we studied wireless-powered communication networks, wherein a set of battery-less devices operate using energy received received from a central node. A network of low-power IoT's or sensors is a typical example of such a scenario. Specifically, we addressed the problem of optimal time allocation for such a network operating in time-division duplexing mode. Furthermore, we also introduced the non-linear effects in energy harvesting devices and their effect on the performance of

proposed algorithms. Simulation results were provided to demonstrate the performance of the proposed algorithms

Related Publications

1. M. P. Deep, S. Jain and P. Ubaidulla, "Relay Selection and Resource Allocation for Energy Harvesting Cooperative Networks," in *2017 IEEE 85th Vehicular Technology Conference (VTC Spring)*, Sydney, NSW, 2017.

2. M. P. Deep, S. Jain and P. Ubaidulla, "Optimal Resource Allocation and Relay Selection for Self-Sustainable Relaying Networks," in *2017 IEEE 85th Vehicular Technology Conference (VTC Spring*, Sydney, NSW, 2017.

Bibliography

[1] L. R. Varshney, "Transporting information and energy simultaneously," in *2008 IEEE International Symposium on Information Theory*. IEEE, 2008, pp. 1612–1616.

[2] P. Grover and A. Sahai, "Shannon meets tesla: Wireless information and power transfer." in *ISIT*, 2010, pp. 2363–2367.

[3] X. Zhou, R. Zhang, and C. K. Ho, "Wireless information and power transfer: Architecture design and rate-energy tradeoff," *IEEE Transactions on Communications*, vol. 61, no. 11, pp. 4754–4767, 2013.

[4] Z. Fang, X. Yuan, and X. Wang, "Distributed energy beamforming for simultaneous wireless information and power transfer in the two-way relay channel," *IEEE Signal Processing Letters*, vol. 22, no. 6, pp. 656–660, 2015.

[5] Y. Zeng and R. Zhang, "Full-duplex wireless-powered relay with self-energy recycling," *IEEE Wireless Communications Letters*, vol. 4, no. 2, pp. 201–204, 2015.

[6] T. Wang, A. Cano, G. B. Giannakis, and J. N. Laneman, "High-performance cooperative demodulation with decode-and-forward relays," *IEEE Transactions on Communications*, vol. 55, no. 7, pp. 1427–1438, 2007.

[7] Y. Rong, X. Tang, and Y. Hua, "A unified framework for optimizing linear nonregenerative multicarrier mimo relay communication systems," *IEEE Transactions on Signal Processing*, vol. 57, no. 12, pp. 4837–4851, 2009.

[8] P. Ubaidulla and S. Aissa, "Optimal relay selection and power allocation for cognitive two-way relaying networks," *IEEE Wireless Communications Letters*, vol. 1, no. 3, pp. 225–228, 2012.

[9] M. Chen and A. Yener, "Multiuser two-way relaying: detection and interference management strategies," *IEEE Transactions on Wireless Communications*, vol. 8, no. 8, pp. 4296–4305, August 2009.

[10] A. A. Nasir, X. Zhou, S. Durrani, and R. A. Kennedy, "Throughput and ergodic capacity of wireless energy harvesting based df relaying network," in *2014 IEEE International Conference on Communications (ICC)*. IEEE, 2014, pp. 4066–4071.

[11] S. T. Shah, D. Munir, M. Y. Chung, and K. W. Choi, "Information processing and wireless energy harvesting in two-way amplify-and-forward relay networks," in *2016 IEEE 83rd Vehicular Technology Conference (VTC Spring)*, May 2016, pp. 1–5.

[12] S. Gautam, E. Lagunas, S. Chatzinotas, and B. Ottersten, "Resource allocation and relay selection for multi-user ofdm-based cooperative networks with swipt," in *2018 15th International Symposium on Wireless Communication Systems (ISWCS)*, Aug 2018, pp. 1–5.

[13] S. Gautam, T. X. Vu, S. Chatzinotas, and B. Ottersten, "Joint wireless information and energy transfer in cache-assisted relaying systems," in *2018 IEEE Wireless Communications and Networking Conference (WCNC)*, April 2018, pp. 1–6.

[14] A. Kurs, A. Karalis, R. Moffatt, J. D. Joannopoulos, P. Fisher, and M. Soljačić, "Wireless power transfer via strongly coupled magnetic resonances," *science*, vol. 317, no. 5834, pp. 83–86, 2007.

[15] T. D. P. Perera, D. N. K. Jayakody, S. K. Sharma, S. Chatzinotas, and J. Li, "Simultaneous wireless information and power transfer (swipt): Recent advances and future challenges," *IEEE Communications Surveys Tutorials*, vol. 20, no. 1, pp. 264–302, Firstquarter 2018.

[16] A. Massa, G. Oliveri, F. Viani, and P. Rocca, "Array designs for long-distance wireless power transmission: State-of-the-art and innovative solutions," *Proceedings of the IEEE*, vol. 101, no. 6, pp. 1464–1481, June 2013.

[17] S. Kim, R. Vyas, J. Bito, K. Niotaki, A. Collado, A. Georgiadis, and M. M. Tentzeris, "Ambient rf energy-harvesting technologies for self-sustainable standalone wireless sensor platforms," *Proceedings of the IEEE*, vol. 102, no. 11, pp. 1649–1666, Nov 2014.

[18] K. W. Choi, D. I. Kim, and M. Y. Chung, "Received power-based channel estimation for energy beamforming in multiple-antenna rf energy transfer system," *IEEE Transactions on Signal Processing*, vol. 65, no. 6, pp. 1461–1476, March 2017.

[19] S. M. Noghabaei, R. L. Radin, Y. Savaria, and M. Sawan, "A high-efficiency ultra-low-power cmos rectifier for rf energy harvesting applications," in *2018 IEEE International Symposium on Circuits and Systems (ISCAS)*, May 2018, pp. 1–4.

[20] M. Kurvey and A. Kunte, "Design and optimization of stepped rectangular antenna for rf energy harvesting," in *2018 International Conference on Communication information and Computing Technology (ICCICT)*, Feb 2018, pp. 1–4.

[21] J. A. G. Akkermans, M. C. van Beurden, G. J. N. Doodeman, and H. J. Visser, "Analytical models for low-power rectenna design," *IEEE Antennas and Wireless Propagation Letters*, vol. 4, pp. 187–190, 2005.

[22] Z. Hameed and K. Moez, "A 3.2 v–15 dbm adaptive threshold-voltage compensated rf energy harvester in 130 nm cmos," *IEEE Transactions on Circuits and Systems I: Regular Papers*, vol. 62, no. 4, pp. 948–956, 2015.

[23] L. Liu, R. Zhang, and K.-C. Chua, "Wireless information and power transfer: A dynamic power splitting approach," *IEEE Transactions on Communications*, vol. 61, no. 9, pp. 3990–4001, 2013.

[24] F. Jameel, A. Ali, and R. Khan, "Optimal time switching and power splitting in swipt," in *Multi-Topic Conference (INMIC), 2016 19th International*. IEEE, 2016, pp. 1–5.

[25] M. Peer, T. Kalluri, V. A. Bohara, D. B. da Costa, and U. S. Dias, "A time-splitting cooperative spectrum sharing amplify-and-forward relaying protocol with energy harvesting cognitive user," in *Wireless and Microwave Technology Conference (WAMICON), 2017 IEEE 18th*. IEEE, 2017, pp. 1–6.

[26] Z. Ding, C. Zhong, D. W. K. Ng, M. Peng, H. A. Suraweera, R. Schober, and H. V. Poor, "Application of smart antenna technologies in simultaneous wireless information and power transfer," *IEEE Communications Magazine*, vol. 53, no. 4, pp. 86–93, April 2015.

[27] R. Zhang and C. K. Ho, "Mimo broadcasting for simultaneous wireless information and power transfer," *IEEE Transactions on Wireless Communications*, vol. 12, no. 5, pp. 1989–2001, 2013.

[28] D. A. Roberson, C. S. Hood, J. L. LoCicero, and J. T. MacDonald, "Spectral occupancy and interference studies in support of cognitive radio technology deployment," in *2006 1st IEEE Workshop on Networking Technologies for Software Defined Radio Networks*, Sept 2006, pp. 26–35.

[29] Y. Zou, Y.-D. Yao, and B. Zheng, "Outage probability analysis of cognitive transmissions: Impact of spectrum sensing overhead," *IEEE Transactions on Wireless Communications*, vol. 9, no. 8, pp. 2676–2688, 2010.

[30] S. Lee, R. Zhang, and K. Huang, "Opportunistic wireless energy harvesting in cognitive radio networks," *IEEE Transactions on Wireless Communications*, vol. 12, no. 9, pp. 4788–4799, September 2013.

[31] S. A. Mousavifar, Y. Liu, C. Leung, M. Elkashlan, and T. Q. Duong, "Wireless energy harvesting and spectrum sharing in cognitive radio," in *Vehicular Technology Conference (VTC Fall), 2014 IEEE 80th*. IEEE, 2014, pp. 1–5.

[32] S. Park, H. Kim, and D. Hong, "Cognitive radio networks with energy harvesting," *IEEE Transactions on Wireless communications*, vol. 12, no. 3, pp. 1386–1397, 2013.

[33] J. He, S. Guo, F. Wang, and Y. Yang, "Relay selection and outage analysis in cooperative cognitive radio networks with energy harvesting," in *2016 IEEE International Conference on Communications (ICC)*, May 2016, pp. 1–6.

[34] F. Wang and X. Zhang, "Resource allocation for multiuser cooperative overlay cognitive radio networks with rf energy harvesting capability," in *2016 IEEE Global Communications Conference (GLOBECOM)*, Dec 2016, pp. 1–6.

[35] X. Kang, C. K. Ho, and S. Sun, "Full-duplex wireless-powered communication network with energy causality," *IEEE Transactions on Wireless Communications*, vol. 14, no. 10, pp. 5539–5551, 2015.

[36] E. Boshkovska, D. W. K. Ng, N. Zlatanov, and R. Schober, "Practical non-linear energy harvesting model and resource allocation for swipt systems," *IEEE Communications Letters*, vol. 19, no. 12, pp. 2082–2085, 2015.

[37] M. Lallart and D. Guyomar, "An optimized self-powered switching circuit for non-linear energy harvesting with low voltage output," *Smart Materials and Structures*, vol. 17, no. 3, p. 035030, 2008.